LOW-CYCLE CYCLIC FATIGUE PROPERTIES OF NOVEL NICKEL-TITANIUM ROTARY ENDODONTIC INSTRUMENTS IN THE SINGLE- AND DOUBLE-CURVATURES.

by

Frédéric Duke

Health Sciences Diploma, Université de Moncton 1994

DMD, Université Laval 1998

GPR, Peninsula Hospital Center 1999

A THESIS SUBMITTED IN PARTIAL FULFILLMENT OF

THE REQUIREMENTS FOR THE DEGREE OF

MASTER OF SCIENCE

in

THE FACULTY OF GRADUATE AND POSTDOCTORAL STUDIES

(Craniofacial Science)

THE UNIVERSITY OF BRITISH COLUMBIA

(Vancouver)

July 2015

Abstract

Introduction: This *in vitro* study aimed to evaluate and compare the fatigue resistance of ProFile Vortex® (VX) and Vortex Blue® (VB) files in two different artificial double curvature canals (DC1 and DC2) and in an artificial single curvature canal (SC). The bending moment of VX and VB was assessed.

Methods: The bending moment (g·cm) was used to measure flexibility of VX and VB (size 25/.04, length: 25mm) according to ISO 3630-1 specifications. Both files types were tested for cyclic fatigue failure inside canals containing: a single curvature (SC: 60^0 curvature, 5 mm radius) and two canals with different double curvature (DC); [DC1: coronal curvature of 60^0 and 5 mm radius, and apical curvature of 30^0 and 2 mm radius; DC2: coronal curvature of 60^0 and 5 mm radius, and apical curvature of 60^0 and 2 mm radius]. The number of cycles to failure (NCF) was recorded and the fracture surface of all fragments was examined with a scanning electron microscope (SEM) to confirm cyclic fatigue failure and for qualitative analysis of pattern of fracture.

Results: VX and VB followed slightly different trajectories in the identical canals, especially in double curvature canals. The mean bending moment value was significantly lower for VB than for VX ($p < .001$). NCF for the two files were significantly higher in the single curvature canal (SC) compared to the two double curvature canals (DC1 and DC2) ($p < .001$). Of the double curvature canals, the NCF was significant higher in DC1 than in DC2 for VB ($p < .05$) but not for VX ($p > .05$). In the SC group, VB had NCF superior to VX ($p < .05$). In DC1 and DC2 groups, NCF of VX and VB was not statistically different from each other ($p > .05$). Multiple crack origins were observed for

the majority of files fractured in DC1 and DC2 canals. **Conclusions**: DC1 and DC2 canals demonstrated a more stressful and challenging anatomy than the SC canal for VX and VB. In double curvature canals, degree of curvature and radius, and the file's flexibility may affect the mean NCF.

Preface

This thesis is an original, unpublished, and independent work by Frédéric Duke. The manuscript was completely written by Frédéric Duke.

The project was conducted under the supervision of Dr. Ya Shen and Dr. Markus Haapasalo and also the guidance of Dr. Jolanta Aleksejūnienė.

In addition to Dr. Markus Haapasalo, Dr. Ya Shen and myself for being involved in all parts of this research project, this thesis was the result of a collaborative approach involving: Dr. Dorin Ruse (research question), Dr. Tom Troczynski (machining of the canals), Dr. Ahmed Hieawy (bending moment testing), Dr. Zhejun Wang (SEM analysis), Ms. Huimin Zhou, PhD (photo analysis), and Dr. Jolanta Aleksejūnienė and Dr. Christine Berthold (statistical analysis). The relative contribution is as follows: Frédéric Duke (60%), Dr. Ya Shen (20%), Dr. Markus Haapasalo (10%) and research team (10%).

Some illustrations used in this thesis were provided by Dr. Ya Shen, Dr. Markus Haapasalo, Frédéric Duke, and from various articles in the literature. Copyrights were obtained for the use of these articles and are cited throughout this document.

This research project has been the foundation for an article submitted and accepted (June 22nd, 2015) for publication in the Journal of Endodontics. At this date, this article

known as "*Cyclic Fatigue of Profile Vortex and Vortex Blue Nickel-titanium Files in the Single- and Double-curvatures*" has not been assigned to a specific volume or issue.

Table of Contents

Abstract ii

Preface iv

Table of Contents vi

List of Tables ix

List of Figures x

List of Symbols xiii

List of Abbreviations xiv

Acknowledgements xv

Dedication xviii

Chapter 1: Introduction 1

1.1 History of Instruments for Root Canal Therapy 1

1.2 Goals of Endodontic Therapy 2

1.2.1 Access to the Root Canal System 2

1.2.2 Enlargement and Debridement of the Root Canal System 3

1.2.3 Disinfection of the Root Canal System 4

1.2.4 Sealing of the Root Canal System 5

1.3 Dr. Schilder's Root Canal Shaping Objectives 5

1.4 Root Canal Anatomy 6

1.5 Endodontic Hand Instruments 8

1.6 Nickel-Titanium Alloys in Endodontics 9

1.7 Rationale for Using Nickel-Titanium Endodontics Files in Root Canal Treatment 17
1.8 Overview of Nickel-Titanium Endodontic File Development 19
1.9 Study Models for Cyclic Fatigue Testing of Nickel-Titanium Endodontic Rotary Files 23
Chapter 2: Rationale for Experiment 30
2.1 Rationale 30
2.2 Aims of the Study 31
2.3 Study Null Hypotheses 31
Chapter 3: Material and Methods 32
3.1 Experiment Design 34
3.2 Canal Configurations 35
3.2.1 Single Curvature 35
3.2.2 Double Curvature #1 36
3.2.3 Double Curvature #2 36
3.3 Statistical Analysis 37
Chapter 4: Results 40
4.1 Influencing Factors 40
4.1.1 Preconditions for Two-Way ANOVA 40
4.1.1.1 Normal Distribution and Equality of Variances 40
4.1.1.1.1 Number of Cycles to Fatigue Data 40
4.1.1.1.2 File Fragment Length Data 40
4.1.2 Precondition for Student's t-test (unpaired) 41

4.1.2.1 Normal Distribution and Equality of Variances 41

4.1.2.1.1 Bending Moment..... 41

4.1.3 General Significance of the Influencing Factors..... 41

4.1.3.1 Influencing Factor-File Type..... 42

4.1.3.2 Influencing factor-Canal Curvature..... 44

4.1.3.3 Influence of Interaction of Factors-File Type and Canal Curvature. 46

4.1.3.4 Influence of File Type on Bending Moment..... 50

4.1.3.5 Fractographic Examination..... 51

Chapter 5: Discussion 58

Chapter 6: Conclusion..... 65

Bibliography 67

Appendices..... 74

Appendix A - Influencing Factor - File Type..... 74

Appendix B - Influencing factor – Canal Curvature..... 75

Appendix C - Influencing Factor - Interaction of File Type and Canal Curvature 76

Appendix D - Influence of File Type on Bending Moment..... 77

Appendix E - Results Chart 78

List of Tables

Table 1. Descriptive statistics for number of cycles for failure (NCF). 74

Table 2. Descriptive statistics for apical fragment length (mm). 74

Table 3. Descriptive statistics for number of cycles to failure (NCF). 75

Table 4. Descriptive statistics for apical fragment length (mm). 75

Table 5. Descriptive statistics for number of cycles to fatigue (NCF). 76

Table 6. Descriptive statistics for apical fragment length..... 76

Table 7. Descriptive statistics for bending moment (g·cm)..... 77

Table 8. Results chart. 78

List of Figures

Figure 1. Elbow and apical zipping in MB root of tooth #26 (*left*) and ledging of the MB root of tooth #37 (*middle left*). Perforation of tooth #44 (*middle right*) and strip perforation in MB root of #46 (*right*). [Reprinted with permission (7)]. 4

Figure 2. Diagram of double curvature canal in proximal view of mesial root of lower molar. [Reprinted with permission (9)]. 7

Figure 3. Canal curvature calculation as per Schneider (A1 and A2) and Pruett et al. (B1 and B2). [Reprinted with permission (14)]. 8

Figure 4. Illustration of the martensitic transformation and shape memory if NiTi alloy. [Reprinted with permission (20)]. 11

Figure 5. Illustration of the shape memory of NiTi alloy. [Reprinted with permission (20)]. 12

Figure 6. Illustration of the superelasticity of NiTi alloy. [Reprinted with permission (20)]. 12

Figure 7. Stress-strain graph of NiTi alloy. [Reprinted with permission (26)]. 14

Figure 8. Lateral view (*left*) and cross-section (*right*) of Profile Vortex® and Vortex Blue® under SEM. [Reprinted with permission (41)]. 21

Figure 9. Generations of NiTi endodontic files. [Courtesy of Dr. Haapasalo and Dr. Shen]. 23

Figure 10. Examples of rotary NiTi endodontic file fractures under SEM: torsional (*left*) and cyclic fatigue failure (*right*). [Reprinted with permission (42)]. 24

Figure 11. Illustration of file fracture (a) and sample (b) after cyclic fatigue failure. [Reprinted with permission (36)]. 26

Figure 12. Two examples of torsional fracture under SEM. Both images display the typical circular pattern due to the friction of the coronal file fragment when rotating against the immobile apical file fragment.. [Reprinted with permission (45)]. 26

Figure 13. Devices for cyclic fatigue failure testing: A) glass or metal tube, B) inclined plane, C) grooved block-and-rod, D) two-pin jig, E) three-pin jig, and F) custom-machined canals. [Reprinted with permission (47-49, 51, 52)]. 29

Figure 14. Flow chart of experimental design. 34

Figure 15. Diagram of the single curvature canal configuration (*left*), picture of custom-machined canal with Profile Vortex® file inserted (*middle*) and Vortex Blue® (*right*). ... 35

Figure 16. Diagram of the DC1 canal configuration (*left*), picture of custom-machined canal with Profile Vortex® file inserted (*middle*) and Vortex Blue® (*right*). 36

Figure 17. Diagram of the DC2 canal configuration (*left*), picture of custom-machined canal with Profile Vortex® file inserted (*middle*) and Vortex Blue® (*right*). 36

Figure 18. Number of Cycles to Fatigue for Profile Vortex (VX) (25.04) and Vortex Blue (VB) (25.04) when all canal curvatures are combined together [Single curvature (SC), double curvature #1 (DC1) and double curvature #2 (DC2)]. 42

Figure 19. File Fragment Length [mm] for Profile Vortex (VX) (25.04) and Vortex Blue (VB) (25.04) when all canal curvatures are combined together [Single curvature (SC), double curvature #1 (DC1) and double curvature #2 (DC2)]. 43

Figure 20. Number of Cycles to Fatigue for the single curvature (SC), double curvature #1 (DC1) and double curvature #2 (DC2) when all file types are combined together [Profile Vortex (25.04) and Vortex Blue (25.04)]. 44

Figure 21. File Fragment Length [mm] for single curvature (SC), double curvature #1 (DC1) and double curvature #2 (DC2) when all file types are combined together (Profile Vortex (25.04) and Vortex Blue (25.04)). 45

Figure 22. Number of Cycles to Fatigue for Profile Vortex (VX) (25.04) and Vortex Blue (VB) (25.04) in single curvature (SC), double curvature #1 (DC1) and double curvature #2 (DC2). 46

Figure 23. File Fragment Length [mm] for Profile Vortex (VX) (25.04) and Vortex Blue (VB) (25.04) in single curvature (SC), double curvature #1 (DC1) and double curvature #2 (DC2). 48

Figure 24. Bending Moment for Profile Vortex (VX) (25.04) and Vortex Blue (VB) (25.04). 50

Figure 25. Fractographic examination of VX in the single curvature canal. Red arrow indicates crack initiation location. From arrow to line : chevron pattern zone, and beyond line: zone of rapid crack propagation. 52

Figure 26. Fractographic examination of VB in the single curvature canal. Red arrow indicates crack initiation location. From arrow to line : chevron pattern zone, and beyond line: zone of rapid crack propagation. 53

Figure 27. Fractographic examination of VX in the double curvature #1 canal. Red arrow indicates crack initiation location. From arrow to line : chevron pattern zone, and beyond line: zone of rapid crack propagation. 54

Figure 28. Fractographic examination of VB in the double curvature #1 canal. Red arrow indicates crack initiation location. From arrow to line : chevron pattern zone, and beyond line: zone of rapid crack propagation. Notice the cracks were not on same level longitudinaly along the file's length creating a step where the two crack propagation zones meet (yellow arrows). 55

Figure 29. Fractographic examination of VX in the double curvature #2 canal. Red arrow indicates crack initiation location. From arrow to line : chevron pattern zone, and beyond line: zone of rapid crack propagation. 56

Figure 30. Fractographic examination of VB in the double curvature #2 canal. Red arrow indicates crack initiation location. From arrow to line : chevron pattern zone, and beyond line: zone of rapid crack propagation. 57

List of Symbols

°C - degree Celsius

© - copyright

® - registered trademark

List of Abbreviations

A_f - austenite-finish temperature

A_s - austenite-start temperature

CBCT - cone beam computed tomography

CM - controlled-memory

DC1 - double-curvature #1 canal

DC2 - double-curvature #2 canal

DSC - differential scanning calorimetry

g·cm - gram·centimeter

ISO - international standards organization

M_f - martensite-finish temperature

M_s - martensite-start temperature

NiTi - nickel-titanium

Nitinol - nickel-titanium naval ordinance laboratory

NCF - mean number of cycles for cyclic fatigue failure

RPM - rotations per minute

SC - single-curvature canal

SEM - scanning electron microscope

VB - Vortex Blue®

VX - Profile Vortex®

Acknowledgements

To Dr. Jeffrey Coil, as Program Director of UBC Graduate Endodontic Program, for giving me the opportunity to join the program and pursue my dream of becoming an endodontist. You have instilled in me the importance of keeping our professional and personal lives in balance, to be curious and fully explore the opportunities endodontics provides us as a practitioner.

To Dr. Ya Shen, as supervisor of this thesis, for your expert direction of the project, balanced comments and giving me the confidence needed to meet the challenges accompanying the completion of this master's thesis. Your knowledge and contribution to the field of research in endodontic files is astounding and I was reminded at each of our encounters how blessed I have been to be working along your side. As a resident with little research experience, Dr. Shen has always been patient, calm and reassuring whenever I would have any questions or worries about this project. Your quiet way of accomplishing tasks at hand have proved to be an excellent model for me to emulate in future endeavours. As an accomplished researcher, I was always reminded of how approachable you are and how it was easy to exchange ideas with you, all with laughter and mutual respect. Without your continuous support, this thesis would have not been such a success, and I am sincerely grateful for it.

To Dr. Markus Haapasalo, as co-supervisor of this thesis and chair of the Division of Endodontics, for your many thoughtful insights on this project and the opportunity to rub shoulders with a true giant of our endodontic community. Your kindness, wisdom and

unvarying sense of humour are only matched by your intellect and legacy of the body of work in endodontic research. Although in very high demand from your many commitments, you have always been attentive to my requests and made time for quality "one-on-one" discussions. Your genuine interest in my well-being, not only as an endodontic resident but as a person as a whole, has always touched me. I am humbled by your unassuming demeanor despite the many accolades you have received professionally and certainly wish to use this as an example of how to conduct myself on a daily basis.

To Dr. Jolanta Aleksejūnienė, as the completing member of my supervisory committee, thank you for your expertise on conducting proper research, your effectiveness and always friendly approach to our work, you have been a joy to work with.

To Dr. Christine Berthold, as a researcher and colleague, for the incalculable amount of hours you spent listening to my theories about this project and endodontics in general. Your patience, commitment to excellence and willingness to share your knowledge with me has better prepared me for this project and for the realities of private practice of endodontics. I am thankful for all the times spent together these past three years and the continued friendship after the completion of our Endodontic program.

Sincere thanks to the members of the research team for your invaluable contributions.

Lastly, I would like to thank the Canadian Academy of Endodontics and the American Association of Endodontists for their financial support of this project, and Dentsply Tulsa Dental Specialties (especially Mr. Stewart Walline and Mr. John Sanktjohanser) for the donation of files used for this project and your help getting information about these products.

Dedication

To my loving wife, Sally, who has been supportive of my career change and a constant source of strength and encouragement especially during the past three years.

To my mother, Marie-Thérèse, who has sacrificed much so my sister and I could have access to higher education and chase our dreams.

To my grandfather, Gérard, who early in my life planted the seeds of honesty, integrity, pride in one's work and willingness to give a helping hand to someone in need.

Chapter 1: Introduction

1.1 History of Instruments for Root Canal Therapy

Endodontic procedures have been first reported in the late 17th century. These first attempts involved many different primitive theories and techniques. The development of the first endodontic instrument is credited to Edwin Maynard in 1838 and consisted of a filed watch spring (1). Several iterations of endodontic instruments have appeared/disappeared since and have evolved through time until instrument standardization was implemented in the mid-1960's with the contribution of Green, Ingle, Heuer and Sampeck (2). Notably, the files produced after these standardization efforts are probably the most recognized and still popular worldwide today: the stainless steel hand files with constant 2% taper. Varying lengths of the cutting portion of the active section of the file, the geometry/metal composition of the wire blank, various shapes given to the twisted wire (e.g.: reamer, k-file, hedstroem) and different file tips were combined to create different hand file instruments. Gradually the instruments we have come to recognize today were taking shape and a more purposeful development of future generations of files was accomplished.

As the standardization of endodontic files and its accompanying windfall on the new era of file production were taking fold in the early/mid-sixties, Buelher et al. was on the cusp of making a scientific discovery that would radically change how the endodontic community tackled the challenge of cleaning and shaping root canal systems (3, 4). The clinical application of NITINOL (Nickel-Titanium Naval Ordinance Laboratory, Buelher et al. 1961) first reported in the Orthodontic literature in 1978 (5) will be

transferred to the manufacturing of endodontic files as a result of Walia et al. in 1988 (6). The addition of these new nickel-titanium alloys have further expanded the multiple permutations of possible endodontic file designs, created numerous research opportunities and accelerated the rate of new file designs and manufacturing processes.

1.2 Goals of Endodontic Therapy

Once it is determined that a tooth needs a conventional root canal therapy, four main broad objectives (7) are aimed at in order to increase the success rate of the treatment provided. These are: 1) Access to the root canal system, 2) Enlargement and debridement of the root canal system, 3) Disinfection of the root canal system, and finally 4) Sealing of the root canal system and access cavity.

1.2.1 Access to the Root Canal System

Access to the root canal system, although intuitive as a first step of the treatment, is very important and will set the tone for how well the root canal therapy will unfold as the clinician progresses to the subsequent three objectives. In addition to removal of the content of the pulp canal chamber, proper access cavity will permit localization of all canal orifices. Access to all orifices is fundamental as we cannot shape and clean a canal not identified. More so, proper access cavity will benefit the shaping and cleaning procedures and help reduce the potential for file fracture while they are actively cutting the dentine walls in each canal. Files entering a canal orifice not properly exposed to the chamber or entering at significant angles compared to the general long axis of the root canal/root can generate stress in a file that can precipitate its fracture. The access

cavity will also serve as a proper reservoir of irrigant. The presence of irrigant used in endodontics helps shaping and cleaning the root canal due to its lubricant effect and keep dentinal debris in a suspension in the irrigating solution. These reduce the chance of endodontic file fracture during root canal therapy.

1.2.2 Enlargement and Debridement of the Root Canal System

Once canals' orifices have been located and properly addressed, each root canal of the system can be "cleaned and shaped". The mechanical action (either by hand or motor-assisted) of the filing will inherently remove material from the root canal. Depending of the pre-operative status of the root canal system, whether the pulp was vital or not or previously filled with a root canal filling material, mechanical preparation of the root canal will serve some benefits. In the respective order previously presented, the removal of the vital but inflamed pulp, removal of infected dentine or removal of existing root canal filling material will provide a better dentinal surface on which irrigants or other products (e.g..: dentine bonding agents) will exert their action. It must be underlined that the above mentioned beneficial effects of mechanical enlargement of a root canal can be negated should the preparations be over enlarged. In the pursuit of greater canal cleanliness by way of mechanical means, the weakened root structure is more prone to root fracture. Also the risk of iatrogenic root canal alterations, such as ledges or strip perforations (Figure 1, p. 4), or file fracture increase with the use of progressively larger files (7).

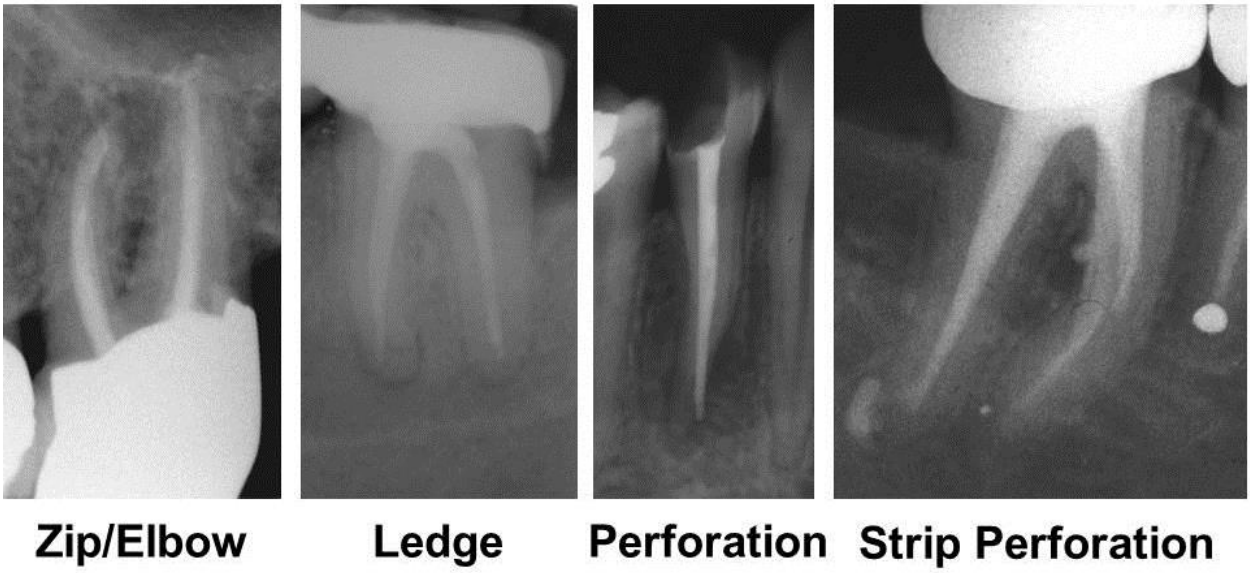

Figure 1. Elbow and apical zipping in MB root of tooth #26 (*left*) and ledging of the MB root of tooth #37 (*middle left*). Perforation of tooth #44 (*middle right*) and strip perforation in MB root of #46 (*right*). [Reprinted with permission (7)].

1.2.3 Disinfection of the Root Canal System

The current materials and methods at our disposal to disinfect the root canal system do not allow their use in an unprepared root canal. The small dimensions of most root canals and the many irregularities in them would prevent the proper action and dispersion of the irrigants currently advocated for proper execution of root canal therapy. The previously mentioned two objectives are mainly serving the purpose of the last two objectives (i.e.: disinfection and obturation of the root canal system). The root canal preparation will aid with the distribution of the various irrigants used to disinfect the root canal system. When no complications are encountered during root canal therapy, cleaning and shaping establishes a reliable and smooth communication from the pulp chamber to the apical terminus of the root canal that permits the clinician to apply their irrigants of choice in order to properly disinfect the canal.

1.2.4 Sealing of the Root Canal System

The root canal preparation and disinfection now completed, the critical goal of preventing reintroduction of pathogenic material in the root canal system from either the coronal or apical aspect of the root canal needs to be finalized. Exemples of coronal reintroduction of pathogens after completion of the root canal therapy would be leakage from a deficient filling in the access cavity or secondary decay reaching the pulp chamber. Apical reintroduction could be encountered when residual pathogens in an apical delta would regain access to the root canal space and spark a periapical inflammatory episode. The current root canal fillings and cements need sufficient space to be properly placed in the root canal and then manipulated to the clinician's desires. As stated earlier, cleaning and shaping also serve the purpose of creating a proper path from the orifice at the floor of the chamber to the apical terminus of the root canal in order to better seal the root canal system tri-dimensionally and prevent reinfection.

1.3 Dr. Schilder's Root Canal Shaping Objectives

Dr. Schilder's undeniable contribution to endodontics is reflected in the five objectives stated below and are still sought for by many clinicians performing root canal therapy (8).

1- A continuously tapering funnel from apex to access cavity.

2- A cross-sectional diameter of the root canal should be narrower at ever point apically.

3- The root canal preparation should flow with shape of the original root canal.

4- The apical foramen should remain in its original position.

5- An apical foramen kept as small as practical.

These guidelines are often used as the benchmark for which a shaped and cleaned root canal is evaluated in order to determine if procedural errors have occurred during the mechanical root canal preparation.

1.4 Root Canal Anatomy

Numerous studies in this regard have documented different shapes and configurations of both the roots and their respective canals. Methods differed greatly from *in vivo* or *ex vivo* radiographic, cleared teeth, or micro-CT studies. Most reports include root canal angulation from a mesio-distal plane, which is most often the only plane visible during the radiographic exam in a clinical setting. Some reports have reported the root canal angulation for a bucco-lingual plane (9-12). This plane is parallel to the x-ray beam and does not offer any information on root canal curvature unless a sufficient horizontal shift during conventional two-dimensional radiography or a three-dimensional image with the aid of cone beam computed tomography (CBCT) is taken. The presence of more than one curvature in a root canal can be unsuspected if the clinician is not alert in seeking such bucco-lingual curvature or they are not obvious when the radiographic exam is performed. Schäfer et al. (12) reported a secondary or “S-shape” canal curvature as high as 59.0% of mesio-buccal root of mandibular second molars (Figure 2, p. 7). Willershausen et al. (10, 11) reported two curvatures in maxillary incisors in 9.7% of the samples examined and between 11.3%-26.0% for either the buccal or palatal root of either the maxillary first or second premolar.

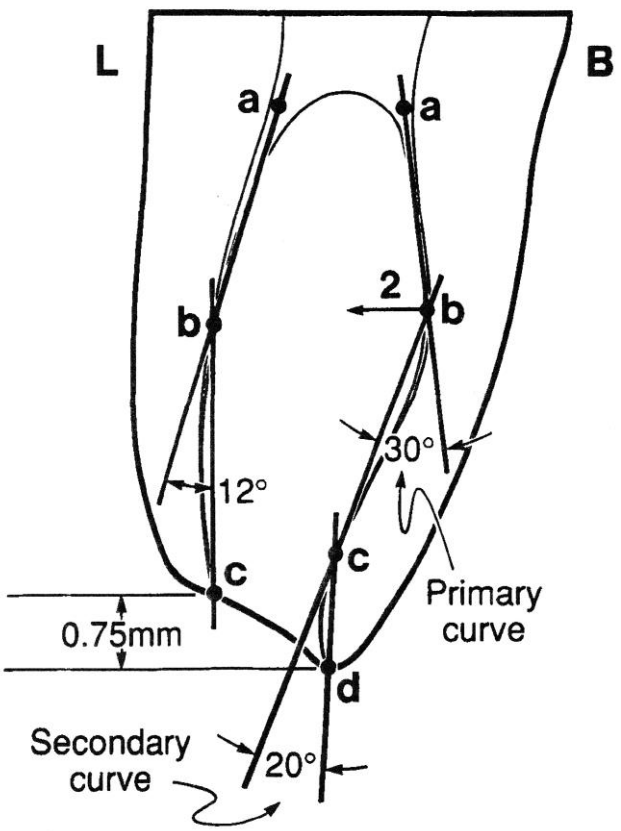

Figure 2. Diagram of double curvature canal in proximal view of mesial root of lower molar. [Reprinted with permission (9)].

A method for measuring root canal curvature has been reported by Schneider in 1971 (13) but modifications of this method by Pruett et al. in 1997 (14) took into account both the angulation and radius of the curvature. The inclusion of these two parameters gives a better representation of the true nature of the root canal encountered (Figure 3, p. 8).

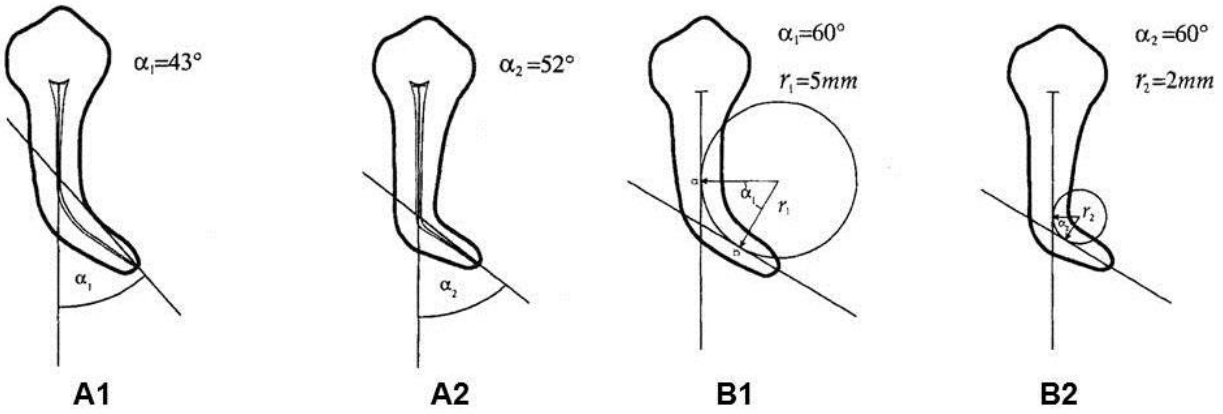

Figure 3. Canal curvature calculation as per Schneider (A1 and A2) and Pruett et al. (B1 and B2). [Reprinted with permission (14)].

1.5 Endodontic Hand Instruments

Since the mid-1960's until the early 1990's, root canal therapy was done in large by traditional stainless steel hand instruments of various lengths, flute designs and methods of use. Although many geometric differences are present within this group of files, they will be discussed as a group in general as they share many handling and mechanical characteristics. Some of these files have been used in a rotary or reciprocating action with the aid of motors but this discussion will concentrate on hand filing.

Stainless steel files are very adequate for straight root canals but present ever mounting challenges when canal curvature increases or other anatomical anomaly (e.g.: S-shaped canal) are encountered in a root canal. The stiffness of these instruments is an advantage when small diameter files are used for negotiating calcified canals, scouting for canal bifurcation below the canal orifice, trying to recapture the root canal anatomy

after ledges, and when used to remove or bypass existing root canal filling (e.g.: gutta-percha, silver points, Thermafill®, etc.) or broken instruments.

As expected, the rigidity of stainless steel files increases as their tip size increases (and consequent overall bulk of the file). Adequate apical size and canal taper after root canal preparations is still a continuous source of debate within the field of endodontics (15-19). But when larger apical sizes are needed in a moderate to severe curved root canal or when difficult anatomy (e.g.: S-shape) is encountered, the use of stainless steel files is more difficult and the possibility of creating an iatrogenic alteration of the canal is also increased. Pre-bending files which will match the root canal curvature is an important skill to master as failure to do so may create deviations from the root canal anatomy such as ledges, zips, perforations or even strip perforations. These root canal alterations will pose potential clinical complications such as: underprepared or uncleaned root canal anatomy, difficulty in creating a proper seal with the root canal filling and sealer, communication of the root canal with the periodontal ligament space, etc. All of these can potentially lower the prognosis of the root canal therapy and make any subsequent improvements more difficult or impossible (7).

1.6 Nickel-Titanium Alloys in Endodontics

Buehler's development of nickel-titanium alloys (Nitinol) for the space program in the early sixties although not applied immediately to the field of endodontics was another landmark step of many leading to the rapid endodontic file development to come (20). Later in 1988, Walia et al. (6) introduced the nickel-titanium alloys as a material to

manufacture endodontic files. Each endodontic file manufacturer closely guard the makeup of their products but the alloys used in endodontics consist usually of 56.0% (54.5%-57.0%) (21) in weight of nickel and 44% of titanium, usually refereed as 55-Nitinol. The file properties can be modified as proportions of each component can vary (where 60.0% nickel/40.0% titanium is referred to 60-Nitinol) or small amount of nickel (less than 2% in weight) can be substituted with cobalt (22), etc. Nickel-titanium alloys have the advantage of an increase in corrosion resistance and strength and lower modulus of elasticity when compared to stainless steel endodontic files. When comparing with same size stainless steel files, nickel-titanium files are more resistant to torsional stress, both in the clockwise and counter-clockwise direction (6). Similarly, nickel-titanium files demonstrate a two to three time increase in flexibility in bending compared to stainless steel files (23, 24). In the more popular 55-Nitinol configuration, the proportion of nickel and titanium used results in a near equiatomic (one-to-one atomic ratio) alloy. The one-to-one atomic ratio and the shifts in the atomic bonding within the alloy permit the nickel-titanium alloy to perform under different crystallographic phases and thus different physical properties. For this reason, nickel-titanium alloys are also characterized as an “intermetallic” alloy. Temperature and mechanical stress on the endodontic file are major influences on which crystallographic form the alloy will adopt (20, 25). Three distinct phases (or crystal structure) are associated with nickel-titanium alloys: 1) austenite, 2) martensite, and 3) transformation phase (or R-phase). Due to the cubic shape of the atoms distribution, the austenitic phase, or parent phase, is the harder and more stable but brittle form of nickel-titanium alloy. When temperature or mechanical stress is applied to a nickel-titanium alloy in its

austenite phase, the atom distribution will be modified into twinned martensite and detwinned deformed martensite (Figure 4, p. 11), (Figure 5, p. 12) and (Figure 6, p. 12).

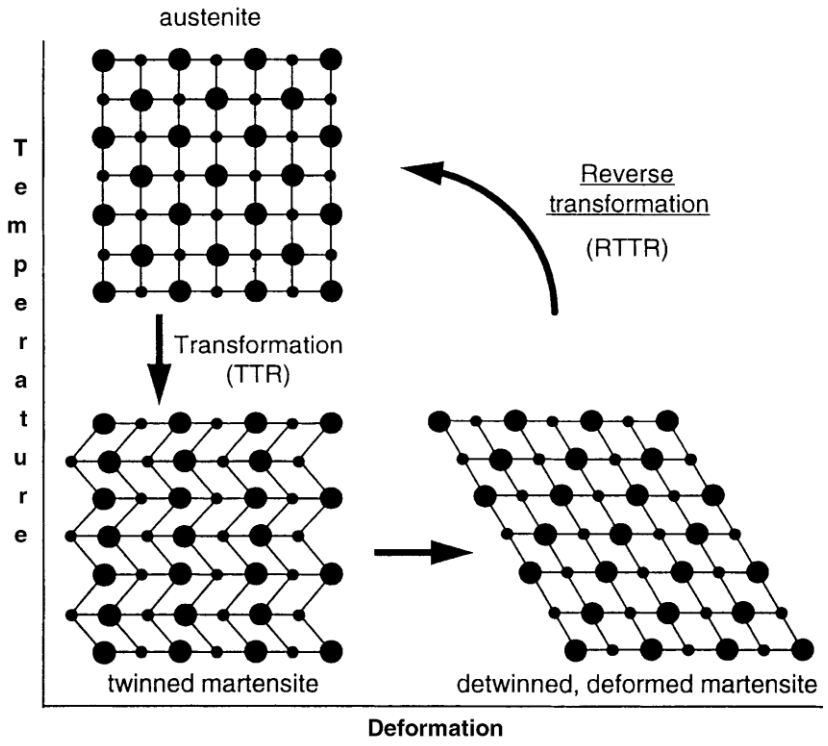

Figure 4. Illustration of the martensitic transformation and shape memory if NiTi alloy. [Reprinted with permission (20)].

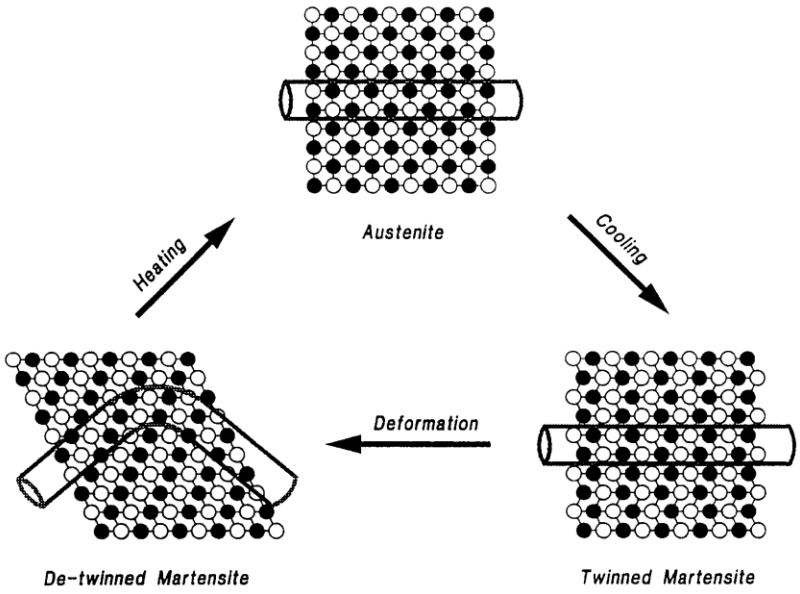

Figure 5. Illustration of the shape memory of NiTi alloy. [Reprinted with permission (20)].

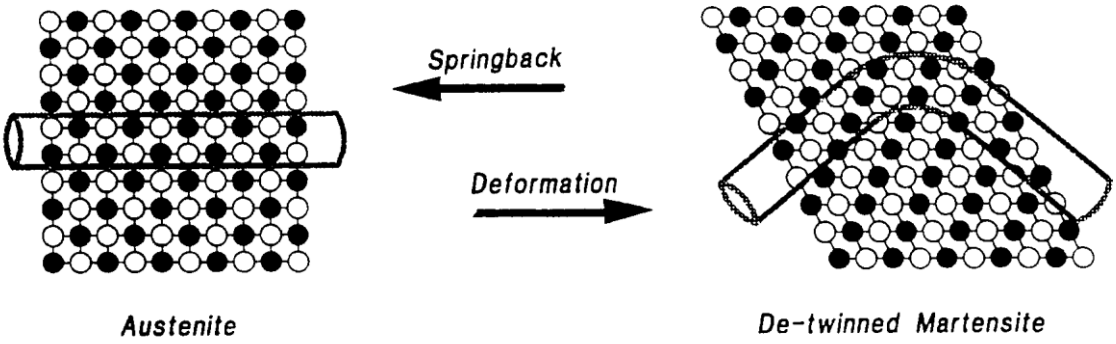

Figure 6. Illustration of the superelasticity of NiTi alloy. [Reprinted with permission (20)].

This martensite phase, or daugther phase, represent a more ductile but less stable form of nickel-titanium alloy. The transition between the true austenite and true martensite form of the nickel-titanium alloy represent the transformation phase, in which the alloy

as a certain amount of both the austenite and martensite phases. This intermediate phase usually gives the endodontic file its superelastic properties. The two most important and notable attributes of nickel-titanium files, due to the continuous transition from one form of the nickel-titanium phase to another, are: superelasticity and shape memory. Superelasticity, the property most utilized of the two previously mentioned, is defined as the leveling of the stress within the endodontic file even though the strain continues to increase (Figure 7, p. 14). The Curve in Figure 7 displays the transition between the three crystallographic forms of a nickel-titanium alloy used for the manufacturing of an endodontic rotary file. In this graph, the first segment of the curve (Strain ~0-2%) represents the alloy in its austenite phase. As the internal stress within the file increases, the alloy transitions into the transformation phase (Strain ~2.0-11.0%). This relatively flat section gives the nickel-titanium file its flexibility and is considered a “safe zone” within which it is preferable to have the alloy in this phase. The third crystallographic phase (martensite) is reached when the strain is over ~11.0% and the instrument will fracture when the strain reaches ~19.0-20.0%. The amount of mechanical stress on the file will influence which crystallographic phase will predominate within the endodontic file. The change from one phase to another fluctuates along with the changes in strain applied to the file.

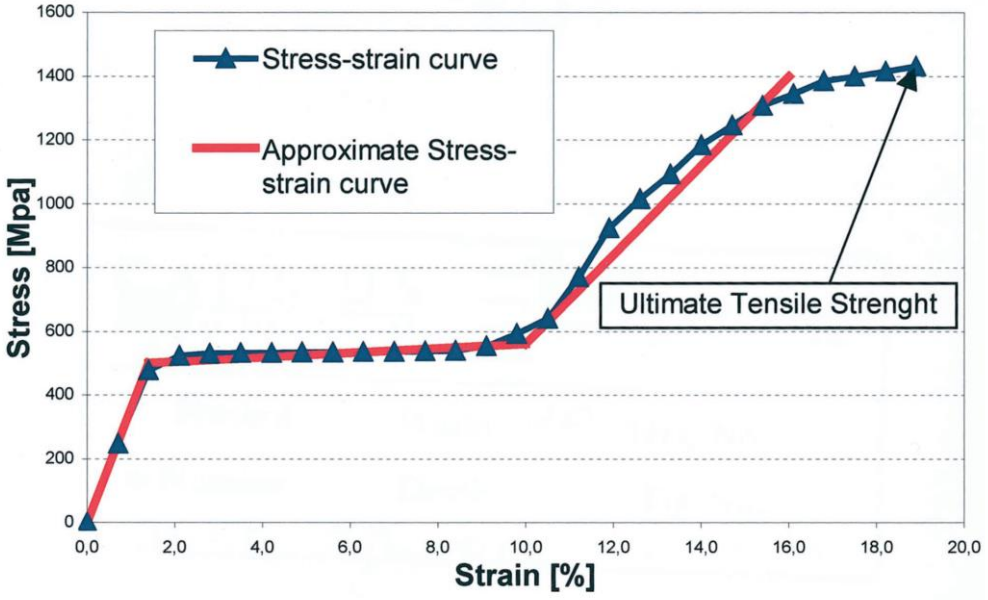

Figure 7. Stress-strain graph of NiTi alloy. [Reprinted with permission (26)].

Shape memory is the capacity of the nickel-titanium file to return to its initial shape, with the aid of heat, after having been strained. Although not significant for the endodontic files tested in this study, shape memory is often encountered when controlled-memory endodontic files have suffered reversible plastic deformation during root canal preparation and is rendered in its normal original shape after going through heat or autoclave sterilization. Further manipulations of the superelasticity and shape memory characteristics of the nickel-titanium alloy in order to enhance or suppress them can be executed during the manufacturing process. As discussed earlier, the precise content of the nickel-titanium alloy can affect the mechanical properties of the future endodontic file. Many different manufacturing processes can alter further these characteristics or improve their resistance to wear or fracture, such as: thermomechanical processing, electropolishing and surface treatment. In regards to the endodontic files used in this research, Profile Vortex® and Vortex Blue® benefit from both thermomechanical

processing via Tulsa Dental's nickel-titanium alloy called M-Wire® (SE508) (25). Vortex Blue® receives further enhancement with a surface treatment consisting of titanium oxide, giving this file its distinctive blue color. Results from recent research projects (27, 28) have helped characterize further the distinctions of Profile Vortex® and Vortex Blue® due to the different thermomechanical treatment they each receive. Shen et al. (28), through the use differential scanning calorimetry (DSC) (29, 30), have made many observations relating to the differences in metallurgy between these two files. Differential scanning calorimetry testing measures the difference in temperature needed to heat and cool the material constituting an endodontic file versus a reference sample. Peaks (or enthalpies) in the data generated by the DSC test indicate the temperatures when a nickel-titanium alloy changes from one crystallographic structure to another, whether on heating or cooling the sample material. These peaks are referred to as austenite-start (A_s), austenite-finish (A_f), martensite-start (M_s), and martensite-finish (M_f) temperatures. Of particular interest is the austenite-finish temperature, which indicates which crystallographic structure of nickel-titanium forms the alloy used for a specific file at room or body temperature. New Profile Vortex® files have an austenite-finish temperature of 53.1°C (28) indicating it is mostly in its martensite form at room/body temperature. This is advantageous as the file is more flexible and able to sustain more strain than the conventional superelastic nickel-titanium endodontic files of the first two file generations which are in their austenite form at room/body temperature. The austenite-finish temperature for new Vortex Blue® files is 38.5°C (28). This A_f temperature is very close to body temperature and would indicate this file would have more austenite and/or R-phase content versus martensite. Shen et al. (28) also report

the presence of one well-defined temperature peak when Profile Vortex ® is either cooled or heated. This indicates a direct transition from martensite to austenite or vice versa (depending if cooling or heating) without passing through the intermediate R-phase. This is similar to Vortex Blue® only when the file was cooled (from austenite to martensite phases) but it displayed two peaks when heated. The first of the two peaks during heating of the Vortex Blue® files indicates the transition from martensite to the R-phase and the second peak, from the R-phase to austenite. The presence of two peaks is explained by the presence of Ni_4Ti_3 resulting from the thermomechanical treatment of Vortex Blue®. This transition and "dwelling period" into the intermediate R-phase before changing to austenite could explain the good performance of Vortex Blue® in NCF tests even when its austenite-finish temperature is close to body temperature and would otherwise normally indicate an alloy mostly in its austenite crystallographic structure. As per Berutti et al. (26), the R-phase (also referred as rhombohedral intermediate phase R or as a premartensitic R-phase) demonstrate many positive attributes in its potential in tolerating large amount of strain without negative repercussions and could be considered to belong within the martensite "family". The R-phase has a lower shear modulus when compared to the austenite and martensite phases and is a transition phase sometimes encountered when an endodontic file passes from austenite to martensite or vice-versa. The knowledge of these processes is proprietary in nature and is closely guarded by the different manufacturers in the dental industry. This is one of the many reasons why many research initiatives involving endodontic files are undertaken across the globe. The results of these research projects give clues on the components of the alloys which helps the

endodontic community understand how dental companies achieve their results. Obviously, each “new and improved” iteration of a specific endodontic file brand is compared with their closest competitors in order to determine if one company offers a more performant product versus their competitor.

1.7 Rationale for Using Nickel-Titanium Endodontics Files in Root Canal Treatment

As previously mentioned, the capacity of stainless steel files to conserve the original curved root canal anatomy is rendered more difficult as the file size increases. The introduction of nickel-titanium alloys into the make-up of the endodontic file solved many of the clinical issues with the use of more traditional endodontic stainless steel files and the techniques used concomitantly with them. Nickel-titanium files have greatly reduced the number or the severity of iatrogenic errors involved in the mechanical shaping of root canals (31, 32). Root canal preparations are generally more centered in the canal and the position of the apical foramen is less affected. The increased cutting efficiency results in time savings and reduction of clinician’s fatigue. The superelastic properties of nickel-titanium files provide a safe way of shaping a canal with a constant taper following the canal anatomy with a larger file taper without sacrificing significantly the original shape of the root canal. Nickel-titanium files are routinely used with constant taper of 2%, 4%, 6% or more or with variable tapers along the length of the same file. They are traditionally used in a continuous rotation but a reciprocating motion has recently been introduced with success. To date, no studies showed any advantage in terms of clinical root canal therapy success, whether the instrumentation was performed

with stainless steel hand files, rotary nickel-titanium files or reciprocating nickel-titanium files (23, 31). After overcoming the initial learning curve of using a rotary nickel-titanium endodontic file system, the clinician can become efficient with its use while decreasing the potential for iatrogenic misadventure during shaping the root canal (33, 34). This is important as it has leveled the playing field amongst the different skills level between practitioners, regardless of being general dentists or endodontists. The many improvements these endodontic files brought with their use did not come without any negative repercussions. One of the first observations of these drawbacks was the file fracture without much warning even though these nickel-titanium files were supposed to be stronger in general when compared to stainless steel files. The fracture of files in constant rotation in the root canals has been attributed to either cyclic fatigue, torsional fatigue, or a combination of both. Other reasons (35, 36) for file fracture can be related to: 1) clinician's lack of experience, 2) manufacturing defect (e.g..: machining defects, crack or bubble in nickel-titanium blank), 3) lack of proper scouting of the root canal and glide path, 4) improper file use not in accordance to manufacturer's recommendations (speed and torque), 5) omission of lubricant, 6) overuse of file in the total number of canal, 7) location of canal curvature in the root canal, its curvature and radius, 8) size of file, etc. Such file fractures are reported to occur in 0.25%-14.0% of cases, with 1.0% of new rotary files fracturing being used often as a measure of their reliability in clinical practice (36, 37). Aside from the embarrassment of the clinician and potential increase in patient treatment time or expenses, these unfortunate events can jeopardize the root canal therapy results (38) or necessitate unplanned procedures such as endodontic surgery to remediate the situation (36, 39). File fragment retrieval causing excess root

dentin removal and blocked canal system apical to the broken file fragment that cannot be properly shaped, cleaned, disinfected and obturated are potential negative consequences of file breakage during the process of root canal therapy. Other negative repercussions noted with the use of rotary nickel-titanium files were possible orifice zipping, due to the surplus of time the file spent rotating in the root canal while wanting regain its original shape. Overzealous use of rotary nickel-titanium files can lead to excess root dentin removal, which can predispose the root to fracture (40). Overall, the advent of rotary nickel-titanium files has raised the level at which most clinician can execute proper root canal shaping and cleaning. But we must remember that the positive progress these files generate in dispensing root canal therapy are not without problems.

1.8 Overview of Nickel-Titanium Endodontic File Development

In 1992, Dr. McSpadden introduced the first rotary instrument for endodontic use but Dr. Johnson's Profile ISO® (Dentsply Tulsa Dental Specialties®) line of rotary files was a resounding commercial success and probably regarded as the prototype identifying the first generation of nickel-titanium rotary files. The main features of these files were the use of the more traditional "superelastic" nickel-titanium alloy, presence of radial lands, constant file taper and a negative rake angle resulting in a scrapping action of dentin instead of a cutting action. The Profile ISO® (Dentsply Tulsa Dental Specialties®) files were the first to take advantage of the greater taper of file (4%) and were known for their canal centering ability (23). At the turn of the new millennium, a second generation appeared on the market. The major differences with the previous generation involved

mainly the lack or reduced use of radial lands, the positive rake angle resulting in an active cutting action and the use of multiple variable file tapers. The archetype file of this generation is Protaper® (Dentsply Tulsa Dental Specialties®) which still enjoys numerous loyal supporters. Two thousand and nine and 2010 brought forward an important development in metallurgical treatment of the nickel-titanium alloys. As stated earlier, these closely guarded industry secrets have shrouded the way theses metals are manipulated but the results have brought on a paradigm shift on the potential use of these files. This third generation focused mainly on metallurgy and less on file geometry. Three major appellations arose from this period, namely: M-Wire® (Dentsply Tulsa Dental Specialties), R-phase (SybronEndo®) and CM Wire® or Controlled-Memory Wire (DS Dental®). These new forms of nickel-titanium alloys displayed greater superelastic qualities compared to the first two generations. Greater flexibility and increased number of cycles for cyclic fatigue failure proved to be the hallmark of these files. This is mainly due to the fact these files are maintained in their martensite phase at room/body temperature. The nickel-titanium alloy of first two generations of files operated mainly in the austenite phase at room/body temperature. Nickel-titanium alloys with greater proportion of martensite phase show more flexibility when compared to files with more austenite phase present. Both Profile Vortex® (Dentsply Tulsa Dental Specialties®) and Vortex Blue® (Dentsply Tulsa Dental Specialties®) studied in this research project are good examples of the third generation of file development (Figure 8, p. 21). Both files share the same triangular cross-section, geometry, design and dimensions. Both are made from M-Wire®. The main distinction between them is the specific and distinct thermomechanical treatment of the nickel-titanium alloy for each

file. The blue surface layer of the Vortex Blue® file is characterized as hard titanium oxide (27). The titanium oxide surface treatment of Vortex Blue® is claimed to increase the file's hardness, flexibility and cutting efficiency. This surface treatment of Vortex Blue® is done after the machining of the file is completed whereas the thermomechanical treatment of Profile Vortex® is done before the machining of the file (i.e. as a wire blank) (28).

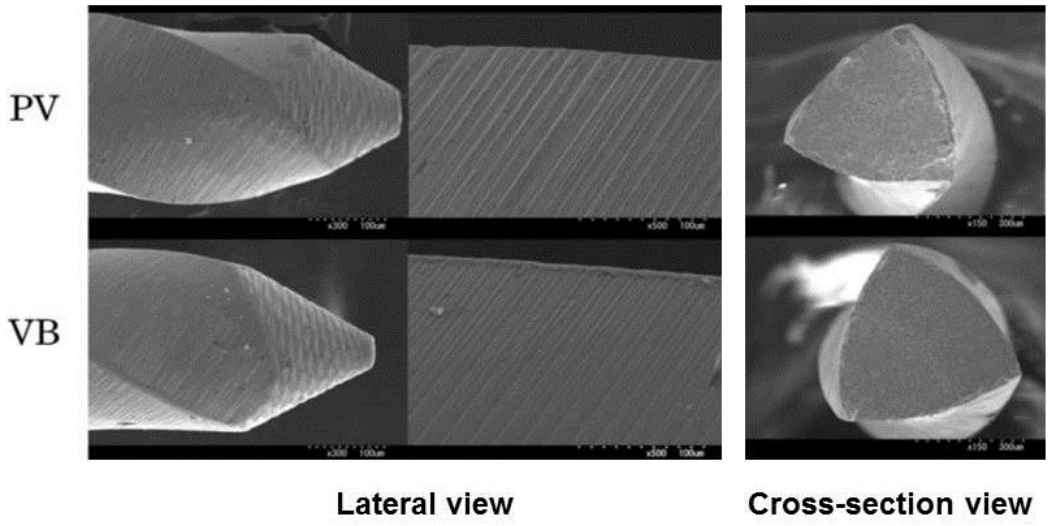

Figure 8. Lateral view (*left*) and cross-section (*right*) of Profile Vortex® and Vortex Blue® under SEM. [Reprinted with permission (41)].

The fourth generation of files is distinctive from the previous three due to its mode of action. Until this moment, engine-driven nickel-titanium files were used in a rotational manner, whereas the fourth generation files, in 2011, are used in a reciprocating movement. This constant clockwise-counterclockwise motion is claimed to follow closely the original path of the root canal and lower the prospect of file fracture by disengaging the tip of the file within the dentin substrate and prolonging the

instrumentation time before failure of the file by way of cyclic fatigue failure. These files share some geometric innovations of the second generation and the metallurgy improvements of the third generations. Examples of this generation are WaveOne® (Dentsply Tulsa Dental Specialties®) and Reciproc® (VDW®). While one could be forgiven for thinking file development reached its peak with little room left for innovative designs, the final and fifth generation of files differentiate themselves with another twist on file geometry. This was accomplished by placing the center of mass of the file off the center of rotation. The “snake-like” motion of the file while in rotation reduces the overall contact of the file on dentin walls, thus reducing the torsional stresses on the file. The manufacturer claims better dentin debris removal and less compaction of dentin mud against the root canal wall. ProTaper Next® (Dentsply Tulsa Dental Specialties®) and TRUShape® (Dentsply Tulsa Dental Specialties®) exemplify files of this latest generation.

Illustrated below are the five generations of engine-driven nickel-titanium endodontic instruments (Figure 9, p. 23).

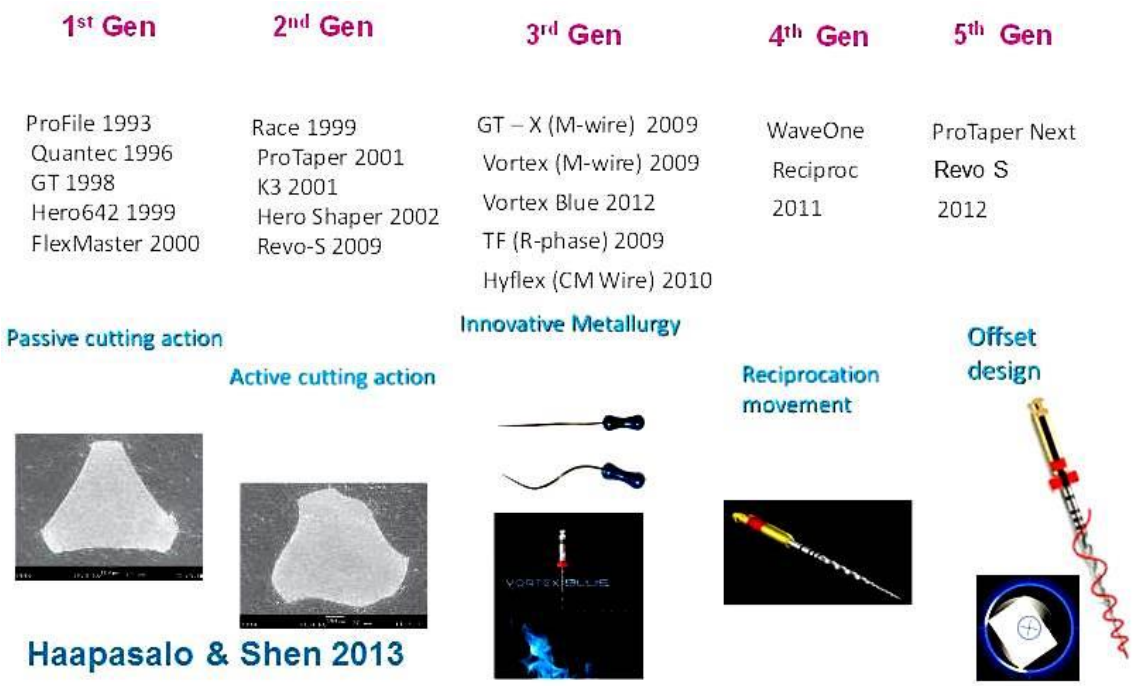

Figure 9. Generations of NiTi endodontic files. [Courtesy of Dr. Haapasalo and Dr. Shen].

1.9 Study Models for Cyclic Fatigue Testing of Nickel-Titanium Endodontic Rotary Files

Since one of the most dreaded clinical adverse events in root canal therapy is related to file fracture, many *in vitro* file studies are related to the evaluation of a specific endodontic file to resist fracture. The results of these studies also serve to extrapolate the *in vivo* performance, margin of safety and to make comparison between different brands. Files fracture mainly by two separate methods: torsional failure and cyclic fatigue. For the sake of eliminating confounding factors and/or ease of conducting the experiment, laboratory studies often focus on one of the two failure mode or a

combination of them when done as separate steps from each other (ex.: torsional test done to certain limits and then do cyclic fatigue testing or vice versa). The actual events leading to a file fracture in a clinical setting most likely involve a simultaneous combination of both torsional and cyclic fatigue failure or at least the influence of one over the other. Torsional failure arises as a result of the tip of the file being locked in the root canal while the remainder of the file continues to rotate until plastic deformation and complete separation of the apical file fragment occurs. One should consider oneself fortunate should you notice plastic deformation of the flutes of the files which serves as a warning sign to discard the file prior to its eminent pending fracture (Figure 10, p. 24).

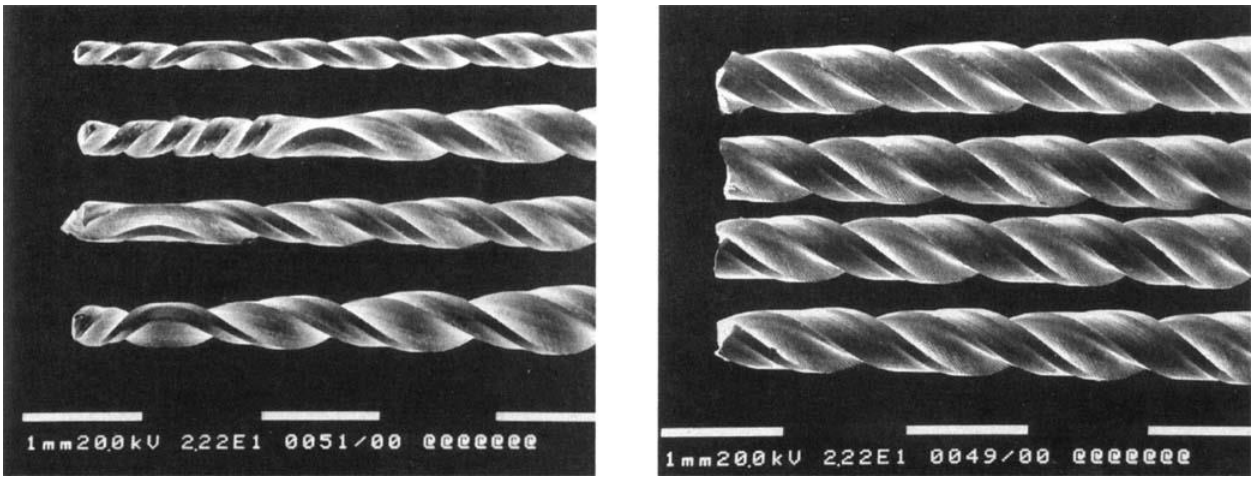

Figure 10. Examples of rotary NiTi endodontic file fractures under SEM: torsional (*left*) and cyclic fatigue failure (*right*). [Reprinted with permission (42)].

Of particular interest for this experiment is the second mode of fracture: cyclic fatigue failure. Cyclic fatigue failure occurs as a result of stress accumulation in a specific area of an endodontic file used in rotation inside a curved root canal. Within the apex of the

curved area of the root canal, the corresponding segment of the endodontic file endures repetitive stress due to the compression of the file on the internal side of the curvature and tension of the file on the external side of the curvature. This could be compared to the bending of a paper clip back and forth until the metal suddenly breaks. This and also the lack of warning signs such as plastic deformation (Figure 10, p. 24) help explain the perplexed reaction of the clinician when such failure occurs in clinical practice, i.e. the sudden and unexpected time when the fracture occurs. Cyclic fatigue failure tests have opened a window explaining partially why and how this phenomenon takes place. Microscopically, cyclic fatigue failure starts at the edge of the file in a zone of concentrated stress. Defects on the cutting edge of the nickel-titanium blank such as a bubble often act as a concentration point for crack initiation (23, 36). The continued cycles of compression-tension on this newly initiated crack slowly and steadily progress toward the core of the file in a slow manner. This area is referred to as chevron pattern. As this crack continues to grow, the proportion of the intact file maintaining its integrity gets smaller. At a certain critical point, this remaining file structure cannot withstand these forces and rapid crack propagation happens resulting in the file's failure. Fractographic examination under scanning electron microscope (SEM) of fractured file fragments is a useful mean of determining which fracture mode the file succumbed to (43). High magnification SEM examination of file fragment fractured due to cyclic fatigue (44) typically show striations in the crack initiation/slow propagation zone and a dimple area (or beach mark) in the rapid fracture propagation area (Figure 11, p. 26).

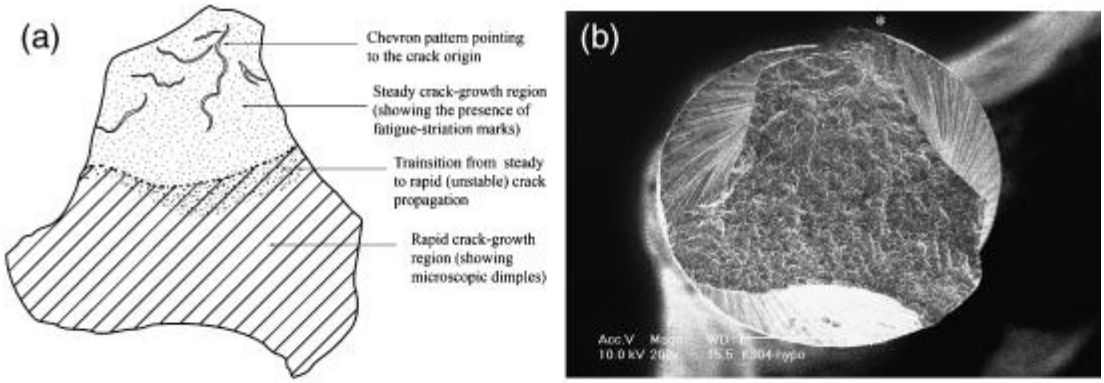

Figure 11. Illustration of file fracture (a) and sample (b) after cyclic fatigue failure. [Reprinted with permission (36)].

Torsional fracture mode is easily distinguished from cyclic fatigue failure. Torsional file fracture often but not always shows signs of plastic deformation when viewed laterally and, under SEM, will reveal itself with a circular pattern of striae resembling grooves on a vinyl record due to the shear stress of the coronal file fragment rotating against its immobile apical portion (45) (Figure 12, p. 26).

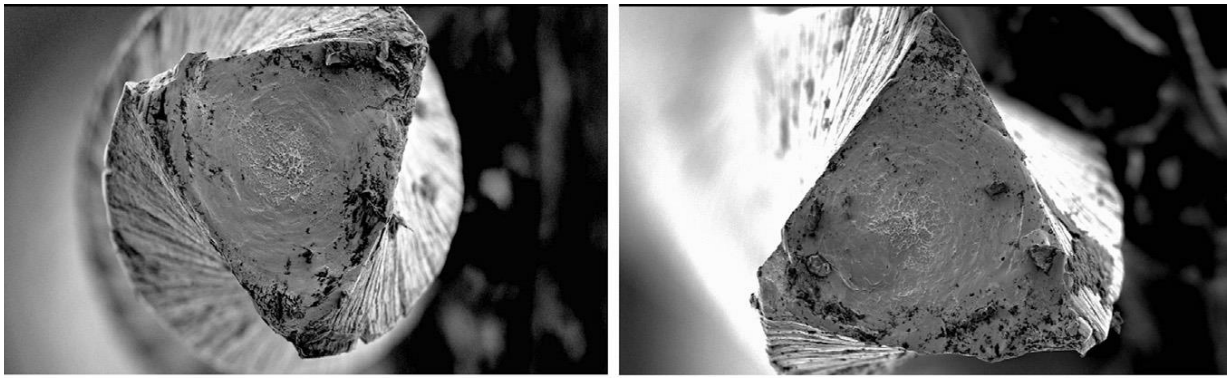

Figure 12. Two examples of torsional fracture under SEM. Both images display the typical circular pattern due to the friction of the coronal file fragment when rotating against the immobile apical file fragment.. [Reprinted with permission (45)].

Regrettably, there are no standards dictating how cyclic fatigue tests are to be conducted. Each research team establishes parameters they find appropriate for their experiment. This renders comparing data from different centers impractical or even impossible. The root canal curvatures and their radiuses used in our machined canals have been influenced by previous studies from this school's research team, other active groups in this field across the globe and our best judgement of what would constitute a realistic and challenging clinical situation. Computer-based Finite Element Analysis (FEA) is sometime used for this purpose but was not considered due to the vast amount of variables that interplay with each other and the difficulty to duplicate a realistic root canal and rotating file inside into a virtual model. Variations of traditional approaches to benchtop experiments have been used in this field (36, 46, 47). Early experiments used a glass or metal tube as a mean to create a "canal". Although practical, different file designs of different sizes would adapt themselves differently inside the tube and thus have slightly different trajectories within the tube. Grooved block-and-rod (48) or inclined planes (49) have been used for placing curvature on a file for cyclic fatigue testing. Both of these methods showed some difficulties in standardizing the file curvatures/ radiuses, keeping the file tip in a desired area without slipping sideways, potential for added friction between the file and the larger surface of contact with the block-rod/inclined plane. As most tests are conducted in a static fashion, the block-rod/inclined plane methods offer the possibility of dynamic testing (49, 50), i.e. vertical movement along the longitudinal axis of the file, to allow simulation of clinical use of an endodontic rotary file when shaping a canal. A two- or three- point jigs (51, 52) have been used to better adjust the file curvature/radius and reduce the friction from the

block-rod and inclined plane models. As previously mentioned with other models, different files adapt themselves in different trajectories when fitted to these jigs. The jigs permit the cyclic fatigue tests to be conducted submerged in a liquid environment of the researcher's choice (ex.: water, sodium hypochlorite, ethylenediaminetetraacetic acid [EDTA]) (51, 53). Finally, Grande et al. (54) have proposed a custom-made canal within a stainless steel block that closely fits the size and shape for each of the tested file (Figure 13, p. 29). Although, confection of the custom-made canals was time-consuming, this permitted the best fit of the files within their respective canal and simultaneously not to be too restrictive as to not induce too much frictional stress on the file (55, 56). This latter method was chosen for our experiment.

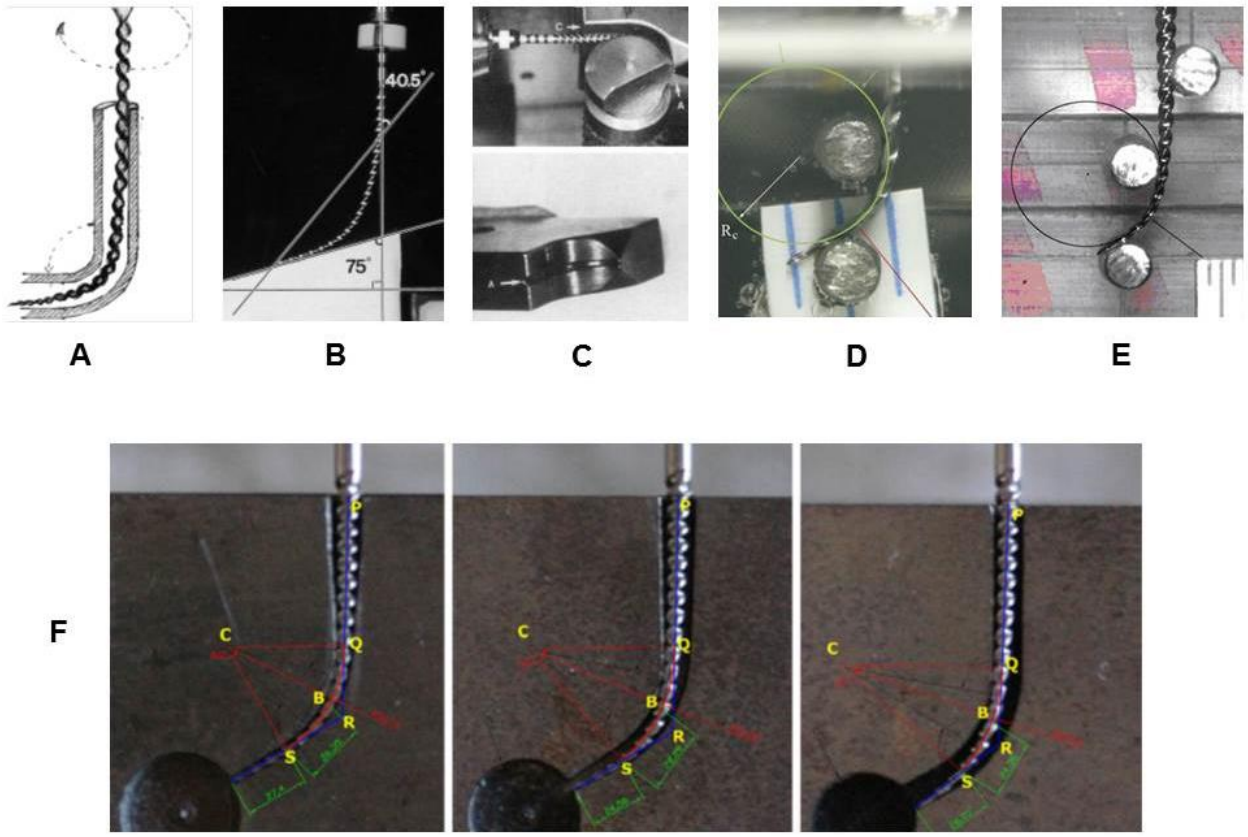

Figure 13. Devices for cyclic fatigue failure testing: A) glass or metal tube, B) inclined plane, C) grooved block-and-rod, D) two-pin jig, E) three-pin jig, and F) custom-machined canals. [Reprinted with permission (47-49, 51, 52)].

The bending moment of each file was performed (ISO specification 3630-1) and recorded using a torsiometer while the file was secured at 3 millimeters from the tip and then bent 45° about their long axis. The bending moments were calculated in order to help interpret the potential trajectory variations within the same canal of same size and identically shaped files but with different thermomechanical treatment of their respective nickel-titanium alloys.

Chapter 2: Rationale for Experiment

2.1 Rationale

Due to rapid acceleration of nickel-titanium rotary file development and their commercial roll-out, the research possibilities are ongoing. The knowledge gap between manufacturers and the endodontic community is still present due to new materials used and/or the manufacturers' innovative methods of processing these materials. The quest to better understand the effect of proprietary thermomechanical treatment of the rotary files certainly warrants further research. With over 22 million endodontic procedures done each year in the United States and an average of rotary file breakage of 1.0% (37), at least 220 000 adverse events of file fracture occur each year. This is a reality today despite acknowledging the latest files' constant improvement of overall clinical performance. Spili et al. (38) found no statistical differences in healing of teeth with lesions of endodontic origin receiving root canal therapy when a file fracture occurs versus when no adverse events. This conclusion is somewhat reassuring but still presents potential for unplanned treatment plan modifications and poses added challenges in regards of prognosis of the tooth in question (39). Another aspect this research will investigate is the effect of two curvatures within one root canal on the mean number of cycles to cyclic fatigue failure (NCF). From the early 1900's Hess demonstrated the complexity of the root canal system and recently, Schäfer et al. have discussed the frequent presence of double curvature within a root canal. They occur most often in bucco-lingual direction thus often going unnoticed. Relatively few studies on file fracture have incorporated the second root canal curvature even though it is known to be a frequent occurrence. The 2012 study on double root canal curvature and

cyclic fatigue failure from Al-Sudani et al. (57) was the first one reported but had some limitations. This study tries to improve on the important work previously mentioned by standardizing: the file geometry and design, similar rotation per minute (RPM) for both files tested, similar but not exact nickel-titanium alloy, more than one canal with a double curvature, measurement of file trajectory in each canal and confirmation of the fracture mode with aid of SEM.

2.2 Aims of the Study

The aims of this study were three-fold: 1) Contribute and expand the current knowledge in regards of nickel-titanium rotary endodontic files and their alloys, specifically with M-wire® and Vortex Blue® technology, 2) Gain information on the impact of two-curvature canals on the number of cycles to obtain cyclic fatigue failure versus a single-curvature canal, and 3) Propose canal configurations with one- and two- curvature in order to put in place a standardized method for cyclic fatigue testing. This last objective would be helpful in establishing external validity to the numerous file testing for cyclic fatigue.

2.3 Study Null Hypotheses

1- Different thermomechanical treatment of the nickel-titanium alloy will not affect the mean number of cycles to cyclic fatigue failure (NCF), and,

2- There is no difference in the mean number in cycles to cyclic fatigue failure (NCF) between single- and double-curvature canals.

Chapter 3: Material and Methods

This experiment used Profile Vortex® (VX) (Dentsply Tulsa Dental Specialities®, Tulsa, OK; lot number: 0000033423) and Vortex Blue® (VB) (Dentsply Tulsa Dental Specialities®, Tulsa, OK; lot number: 0000036516) both in size 25/.04 and 25mm in length.

Flexibility of both VX and VB was measured using the bending test. The bending test was performed using a torsiometer (Sabri Dental Enterprises®, Downers Grove, IL) at room temperature according to the ISO specification 3630-1 (58). Twelve of each instrument were secured at a distance of 3 mm from the tip and then bent 45° about their long axis. The bending moment at an angular deflection of 45º was recorded in grams-centimeters (g.cm).

Cyclic fatigue testing was accomplished using twelve files of both VX and VB for each of the three canal configurations used in this experiment (Figure 14, p. 34). All three artificial canals were milled in the stainless steel plate using a numerical computer control machining bench at a size of 30/.06. Following Pruett and associates' method for measuring canal curvature, an artificial single curvature canal model (SC: 60^0 curvature, 5 mm radius) (Figure 15, p. 35), and two double curvature models [(DC1: coronal curve of 60^0 curvature and 5 mm radius, and an apical curve of 30^0 curvature and 2 mm radius) (Figure 16, p. 36) and (DC2: coronal curve of 60^0 curvature and 5 mm radius, and the apical curve of 60^0 curvature and 2 mm radius) (Figure 17, p. 36)] were created and used for this experiment. A calibrated digital photograph was taken of each

of the curvatures. Stainless steel plates were secured on a jig which also held in place the endodontic handpiece which served to rotate the files. The instruments were rotated at a constant speed of 500 rpm (AEU-20 Endodontic System, Dentsply Tulsa Dental®), at the recommended torque values. To reduce the friction of the file as it made contact with the artificial canal walls, synthetic oil (Boyle Midway®, Toronto, Canada) designed for lubrication of mechanical parts was applied to the canal's internal surfaces. Each file was rotated in the canal until fracture of the file occurred. Time, in seconds (s), needed for file fracture was recorded and was then converted into number of cycles to fracture (NCF) representing fatigue life. The length of the detached fragments was measured in millimeters (mm) using a stereomicroscope at 10X (Microdissection®; Zeiss, Bernried, Germany). The fractured instrument was also cleansed in an ultrasonic bath of absolute alcohol and a fractographic examination was performed on the fractured surface using a scanning electron microscope (SEM) at a magnification of 200-1000X operating at 3-7 kV (Helios NanoLab 650®, FEI, Eindhoven, Netherlands).

Geometrical analysis of the trajectory of each instrument followed inside the artificial canal was performed on the digital images. The angle and radius of the curvature were determined using the osculating circumference method via computer software (ImageJ 1.34n; National Institutes of Health, Bethesda, MD). The angle of curvature was defined as the number of degrees (°) on the arc of the circle between the beginning and end-points of the curvature; the radius of the circle was defined as the radius of the canal curvature in millimeters (mm).

3.1 Experiment Design

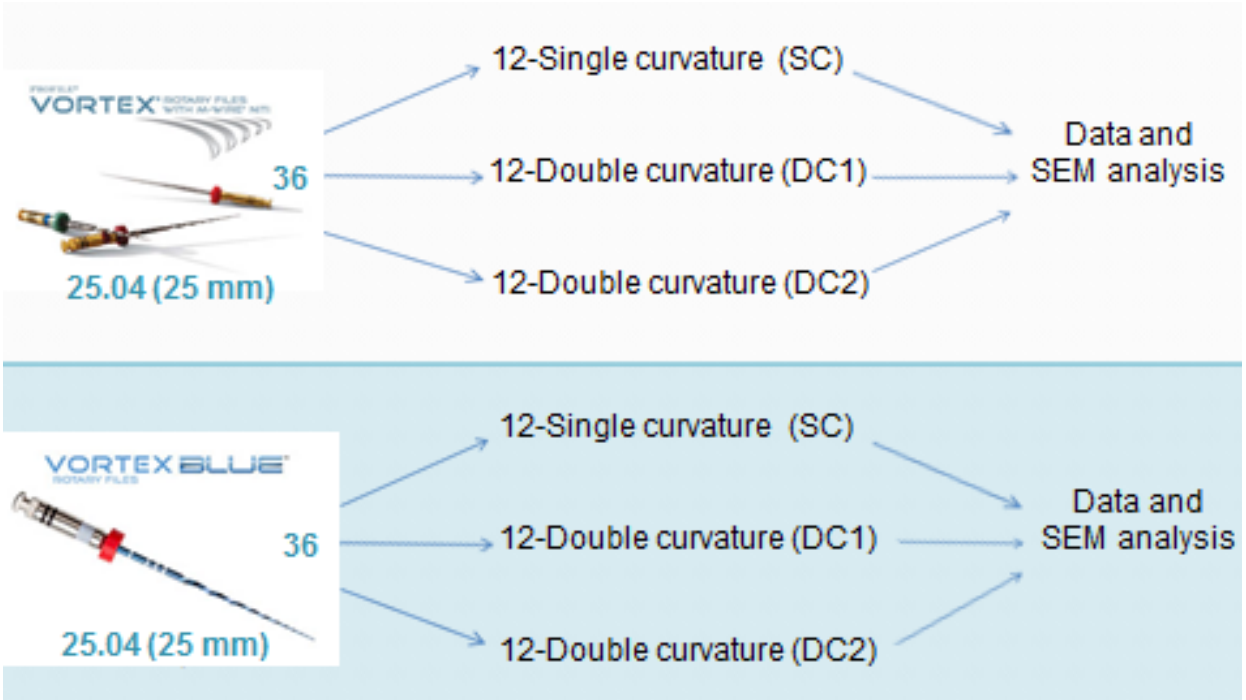

Figure 14. Flow chart of experimental design.

3.2 Canal Configurations

3.2.1 Single Curvature

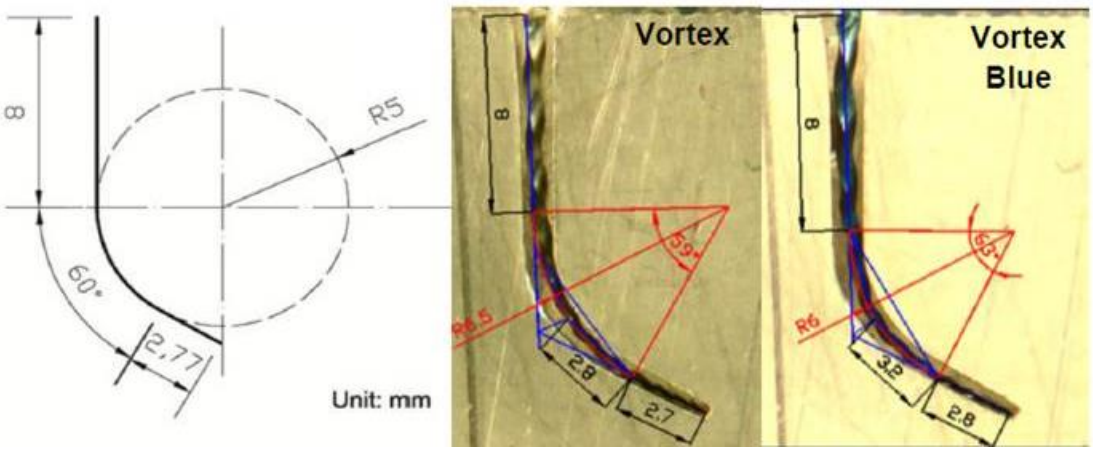

Figure 15. Diagram of the single curvature canal configuration (*left*), picture of custom-machined canal with Profile Vortex® file inserted (*middle*) and Vortex Blue® (*right*).

3.2.2 Double Curvature #1

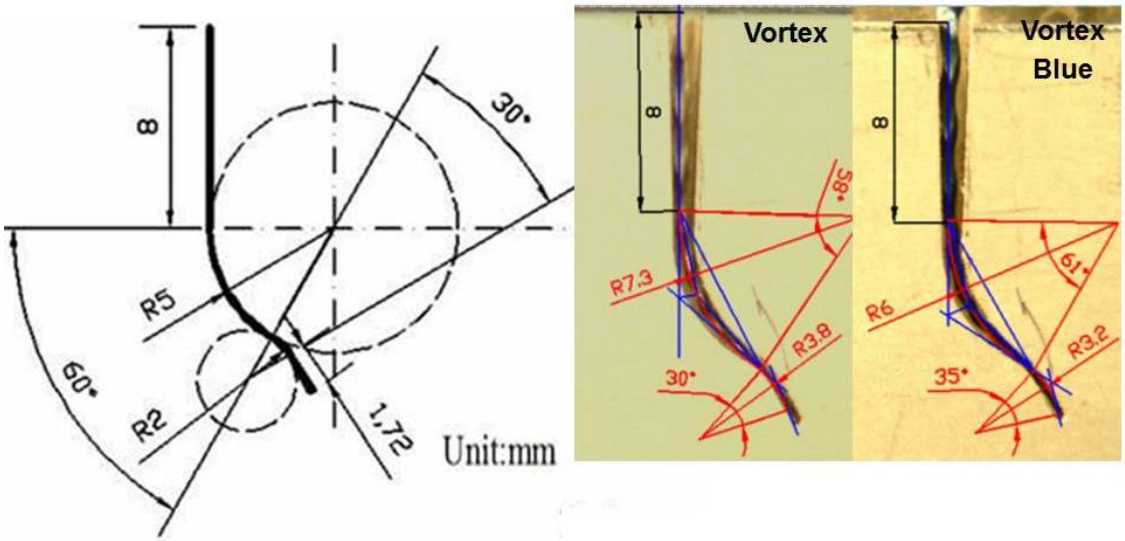

Figure 16. Diagram of the DC1 canal configuration (*left*), picture of custom-machined canal with Profile Vortex® file inserted (*middle*) and Vortex Blue® (*right*).

3.2.3 Double Curvature #2

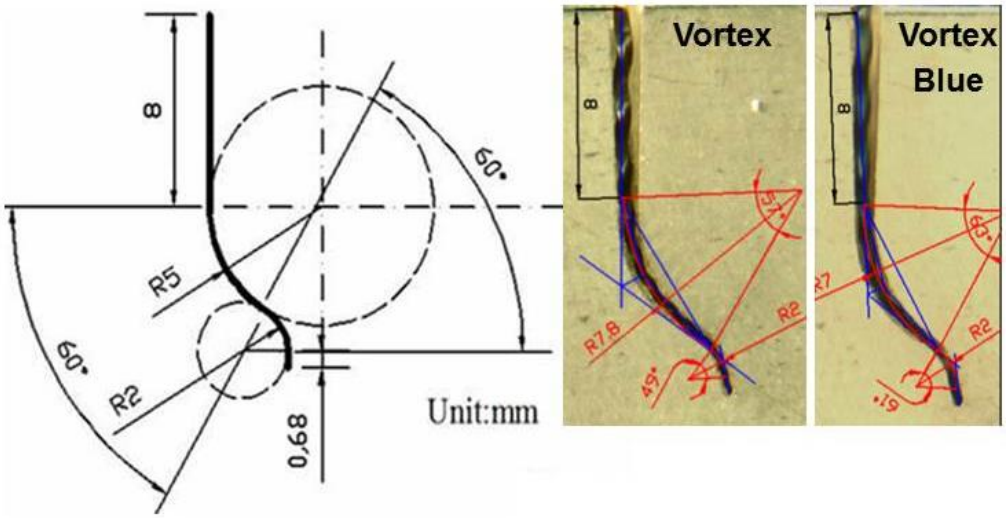

Figure 17. Diagram of the DC2 canal configuration (*left*), picture of custom-machined canal with Profile Vortex® file inserted (*middle*) and Vortex Blue® (*right*).

3.3 Statistical Analysis

The data for the NCF, fragment length and bending moment were analyzed statistically using SPSS 11.0 for Windows (Chicago, IL). The significance level was set at $\alpha=0.05$.

Descriptive Statistics

The data for NCF, fragment length and bending moment were described using mean, median, variance, standard deviation, minimum, maximum and interquartile range.

Diagrams

Results for NCF, fragment length and bending moment are displayed with the aid of box plots.

Normal Distribution

A non-parametric test (Kolmogorov-Smirnov test) was used for the NCF, fragment length and bending moment data to measure presence of normal distribution. P-value > 0.05 signifies normal distribution of the data. In such cases, parametric tests were used for statistical analysis of data. Non-parametric tests were alternatively used when a non-normal distribution of data was found.

Equality of Variance

Evaluation of equality of variance (or variance homogeneity) was conducted with the Levene's test. P-value > 0.05 signifies equality of variance of the data tested and

serves as a precondition for comparison of tests results with parametric tests and for the choice of Post-hoc tests.

Significance of Influencing Factors

The results of the Kolmogorov-Smirnov and Levene's test indicated that Two-Way-ANOVA test could be used to analyze the influence of File Type and Canal Curvature as well as the interaction between the two factors on the NCF data. The results of the Kolmogorov-Smirnov and Levene's test indicated that t-test could be used to analyze the influence of file type on the bending moment. P-value < 0.05 signifies a statistically significant difference between groups tested.

The lack of normal distribution of the fragment length data resulted in the use of the Mann-Whitney-U test for testing the influence of the File Type (VX and VB) and the application of the Kruskal-Wallis test for analyzing the influence of the Canal Curvature (SC, DC1 and DC2). P-value < 0.05 signifies a statistically significant difference between groups tested for both non-parametric tests.

Pairwise Comparison or Post-hoc Tests

For pairwise comparison of the NCF data between the different canal curvature types, Dunnett T3 (no equality of variance) or Bonferroni (equality of variances) post-hoc test was used.

To offset α-error accumulation during multiple testing, the Bonferroni correction was applied to adjust the local significance level α' (α' = α/number of comparisons).

Chapter 4: Results

4.1 Influencing Factors

After assessing the data for normal distribution and their equality of variance, proper statistical tests were chosen to analyze the influence of the factors: file types, canal curvatures, interactions of both factors on the NCF and fragment length, and finally, the bending moment.

4.1.1 Preconditions for Two-Way ANOVA

4.1.1.1 Normal Distribution and Equality of Variances

4.1.1.1.1 Number of Cycles to Fatigue Data

The NCF data displayed normal distribution (Kolmogorov-Smirnov test; $p > 0.05$), and equality of variances (Levene's-test; $p > 0.05$). Therefore, the data was analyzed with parametric tests.

4.1.1.1.2 File Fragment Length Data

The fragment length did not display normal distribution (Kolmogorov-Smirnov test; $p < 0.05$). Therefore, nonparametric test was applied.

4.1.2 Precondition for Student's t-test (unpaired)

4.1.2.1 Normal Distribution and Equality of Variances

4.1.2.1.1 Bending Moment

The bending moment data displayed normal distribution (Kolmogorov-Smirnov test; $p > 0.05$), and equality of variances (Levene's-test; $p > 0.05$). Therefore, the data was analyzed with parametric tests.

4.1.3 General Significance of the Influencing Factors

File type and canal curvature both significantly affected the NCF (Two-Way ANOVA; $p < 0.05$). File fragment length was not significantly affected by file type (Mann-Whitney-U test; $p > 0.05$) but, alternatively, was affected significantly by canal curvature (Kruskal-Wallis test; $p < 0.05$). File type influenced the bending moment (Student's t-test; $p < 0.05$) (Appendix E, Table 8, p. 78).

4.1.3.1 Influencing Factor-File Type

The descriptive data for the file type is presented in Appendix A (Table 1 and Table 2, p. 74).

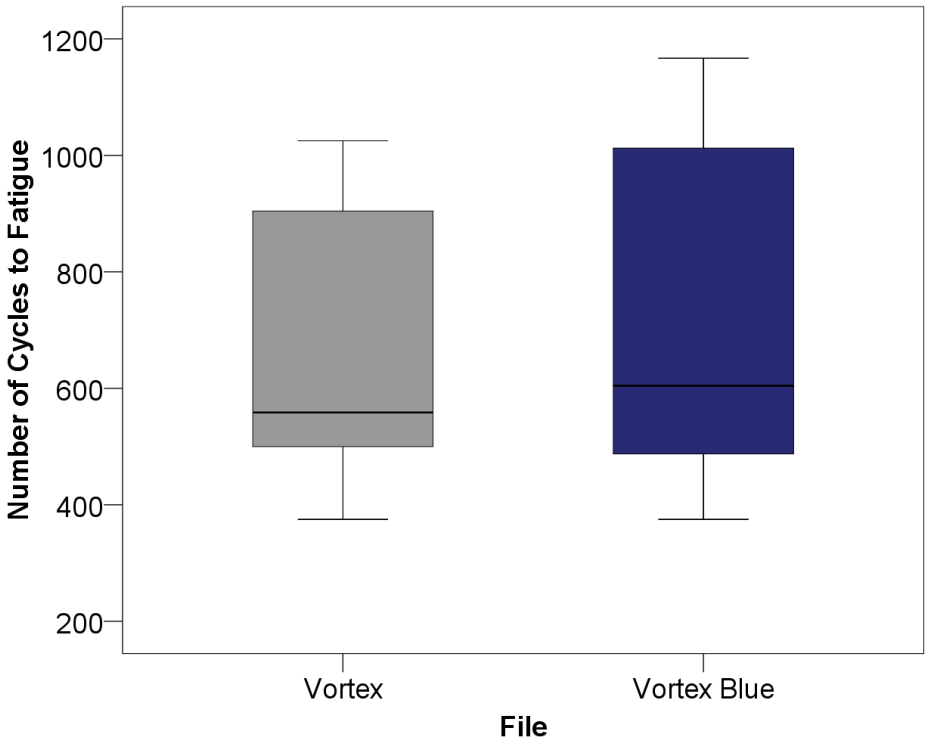

Figure 18. Number of Cycles to Fatigue for Profile Vortex (VX) (25.04) and Vortex Blue (VB) (25.04) when all canal curvatures are combined together [Single curvature (SC), double curvature #1 (DC1) and double curvature #2 (DC2)].

When comparing the two file types, independent of the canal curvature, statistically significant differences were found (Two-way ANOVA ($p < o.o5$), $p = 0.044$). VX had a mean NCF of 660.2 ± 218.4 while VB had a mean NCF of 710.7 ± 261.1 (Figure 18, p. 42).

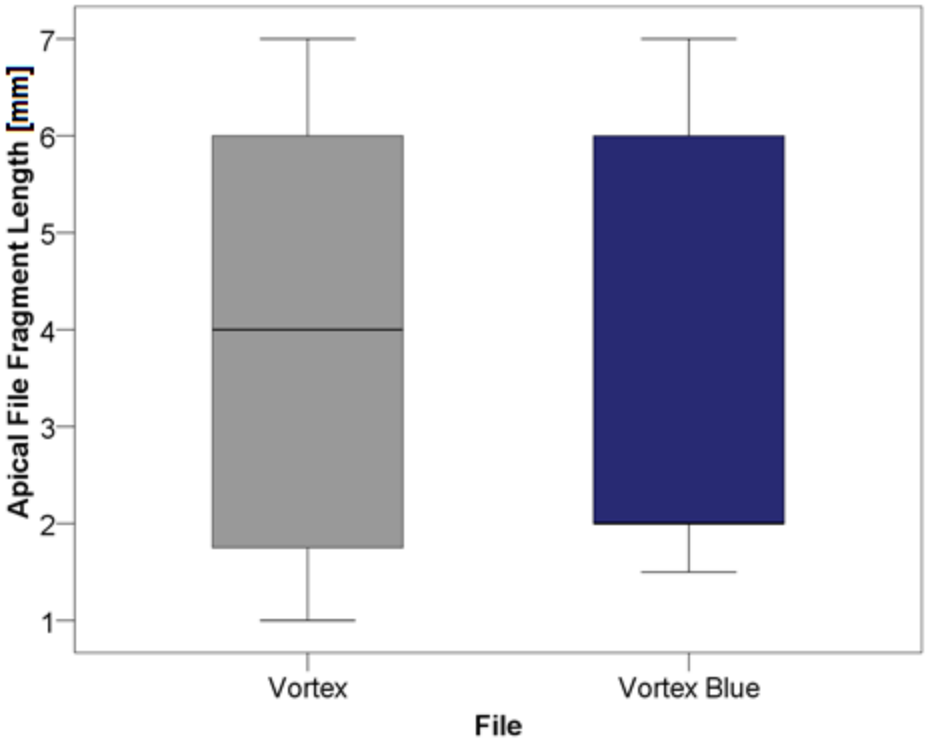

Figure 19. File Fragment Length [mm] for Profile Vortex (VX) (25.04) and Vortex Blue (VB) (25.04) when all canal curvatures are combined together [Single curvature (SC), double curvature #1 (DC1) and double curvature #2 (DC2)].

When comparing the fragment length between the two file types, independent of the canal curvature, no statistically significant difference was detected (Mann-Whitney-U-test ($p < 0.05$), $p = 0.801$). VX had a mean file fragment length of 4.0 ± 2.3mm and VB had a mean file fragment length of 3.4 ± 2.0mm (Figure 19, p. 43).

4.1.3.2 Influencing factor-Canal Curvature

The descriptive data for the canal curvature is presented in Appendix B (Table 3 and Table 4, p. 75).

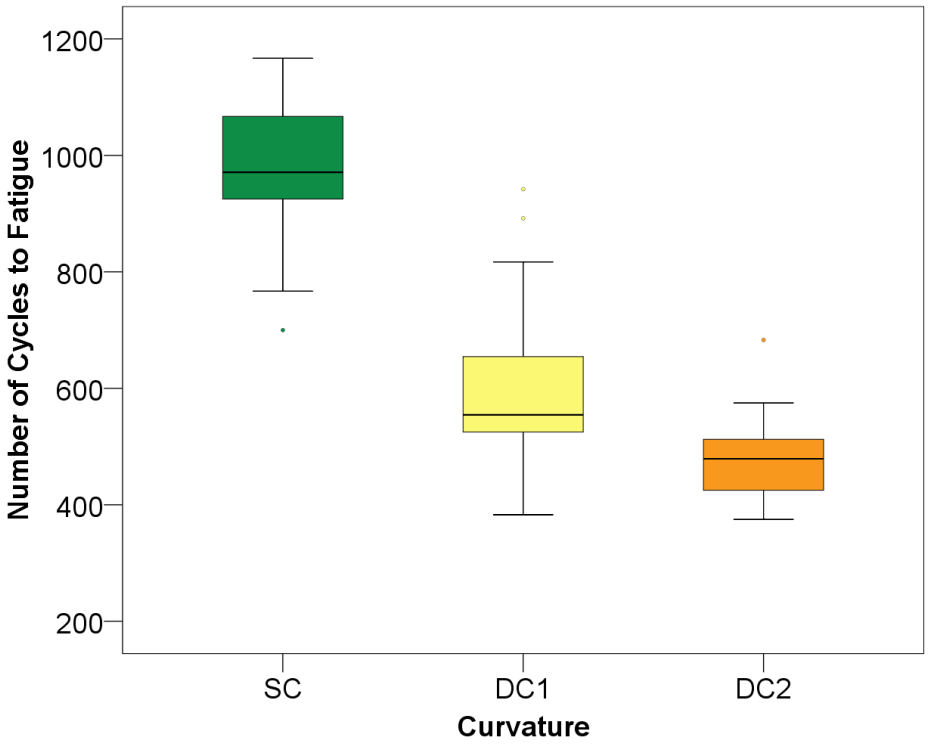

Figure 20. Number of Cycles to Fatigue for the single curvature (SC), double curvature #1 (DC1) and double curvature #2 (DC2) when all file types are combined together [Profile Vortex (25.04) and Vortex Blue (25.04)].

When comparing the three canal curvatures, independent of the file type, statistically significant differences were found between SC and DC1 (Bonferroni post-hoc test, $p < 0.001$), between SC and DC2 (Bonferroni post-hoc test, $p < 0.001$) and between DC1 and DC2 (Bonferroni post-hoc test, $p = 0.001$). SC had a mean NCF of 978.5 ± 108.7,

while DC1 had a mean NCF of 598.4 ± 139.4 and DC2 had a mean NCF of 479.5 ± 72.3 (Figure 20, p. 44).

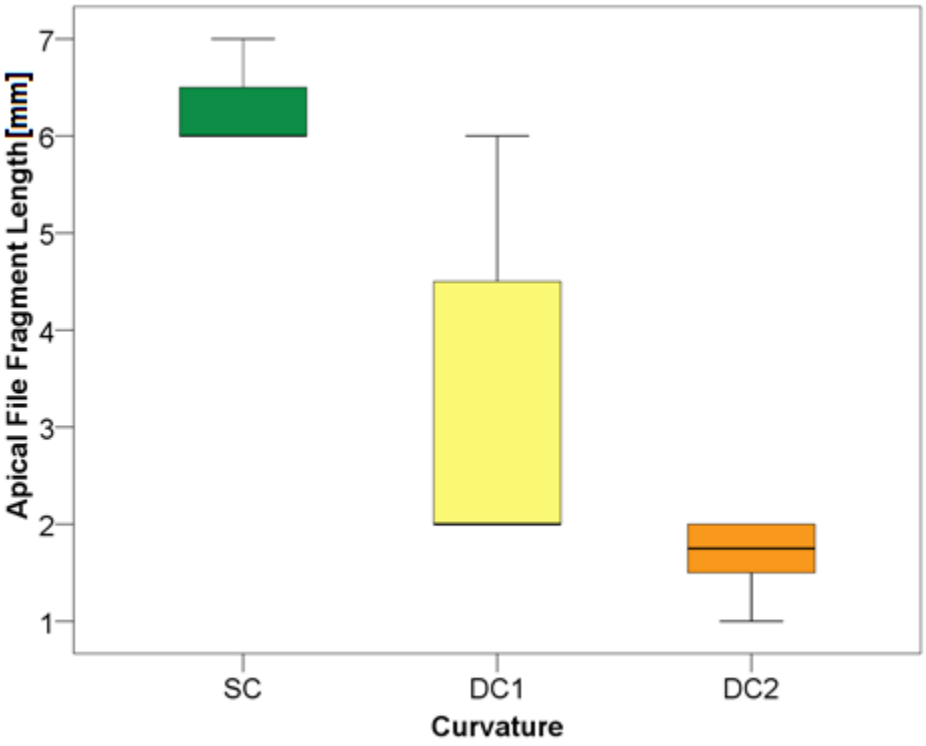

Figure 21. File Fragment Length [mm] for single curvature (SC), double curvature #1 (DC1) and double curvature #2 (DC2) when all file types are combined together (Profile Vortex (25.04) and Vortex Blue (25.04)).

When comparing the three canal curvatures, independent of the file type, statistically significant differences were found between SC and DC1 (Mann-Whitney-U-test, $p < 0.001$), between SC and DC2 (Mann-Whitney-U-test, $p < 0.001$) and between DC1 and DC2 (Mann-Whitney-U-test, $p < 0.001$). SC had a mean fragment length of 6.3 ±

0.4mm, while DC1 had a mean file fragment of 3.1 ± 1.7mm and DC2 had a mean file fragment of 1.7 ± 0.3mm (Figure 21, p. 45).

4.1.3.3 Influence of Interaction of Factors-File Type and Canal Curvature.

The descriptive data for the interaction of factors file type and canal curvature is presented in Appendix C (Table 5 and Table 6, p. 76).

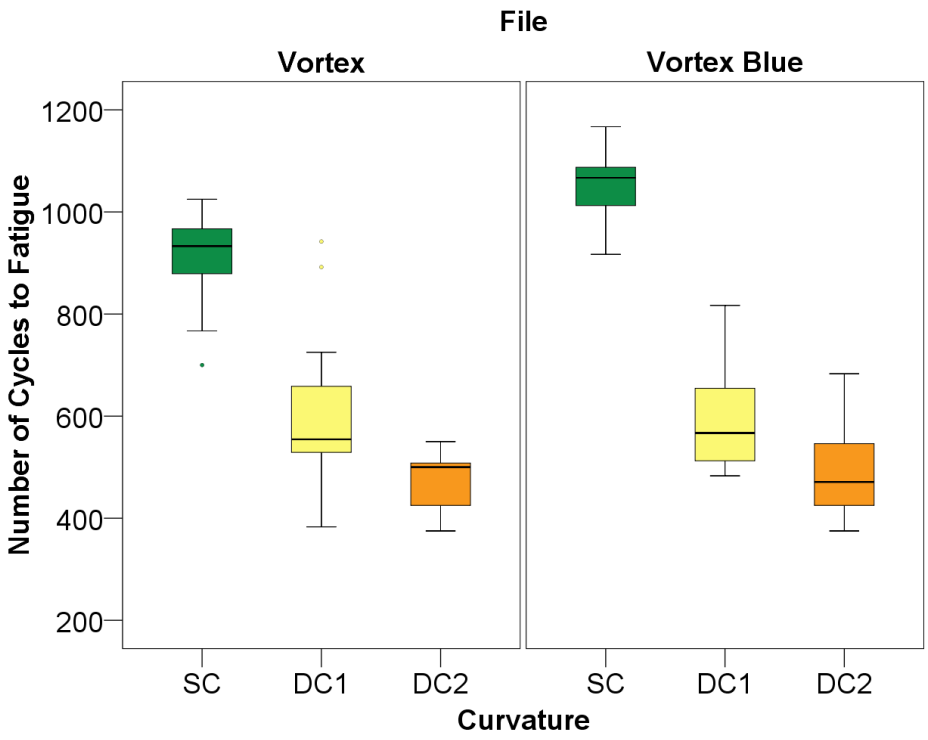

Figure 22. Number of Cycles to Fatigue for Profile Vortex (VX) (25.04) and Vortex Blue (VB) (25.04) in single curvature (SC), double curvature #1 (DC1) and double curvature #2 (DC2).

Profile Vortex files

The canal curvature significantly influences the NCF (Welch-test; $p < 0.001$). Pairwise comparisons showed statistically significant differences between SC and DC1 and between SC and DC2 (Dunnett T3; $p < 0.05$) but not for the comparison between DC1 and DC2 (Dunnett T3; $p > 0.05$). SC had a mean NCF of 908.3 ± 92.4, while DC1 had a mean NCF of 602.2 ± 172.2 and DC2 had a mean NCF of 470.1 ± 57.7 (Figure 22, p. 46).

The canal curvature significantly influences the file fragment length (Kruskal-Wallis test; $p < 0.001$). Pairwise comparisons at the adjusted significance level (Bonferroni correction; $\alpha' = 0.016$) showed statistically significant differences between SC and DC1, between SC and DC2, and between DC1 and DC2 (Mann-Whitney-U test; $p < 0.016$). Mean file fragment length for SC was 6.4 ± 0.4mm, mean file fragment length for DC1 was 4.0 ± 2.1mm and mean file fragment length for DC2 was 1.5 ± 0.3mm (Figure 23, p. 48).

Vortex Blue files

The canal curvature significantly influences the NCF (Welch-test; $p < 0.001$). Pairwise comparisons showed statistically significant differences between SC and DC1, between SC and DC2, and between DC1 and DC2 (Dunnett T3; $p < 0.05$). SC had a mean NCF of 1048.7 ± 73.7, while DC1 had a mean NCF of 594.6 ± 104.6 and DC2 had a mean NCF of 488.8 ± 86.1 (Figure 22, p. 46).

The canal curvature significantly influences the file fragment length (Kruskal-Wallis test; $p < 0.001$). Pairwise comparisons at the adjusted significance level (Bonferroni correction; $\alpha' = 0.016$) showed statistically significant differences between SC and DC1 and between SC and DC2 (Mann-Whitney-U test; $p < 0.016$) but not between DC1 and DC2 (Mann-Whitney-U test; $p > 0.016$). Mean file fragment length for SC was 6.2 ± 0.3mm, mean file fragment length for DC1 was 2.1 ± 0.3mm and mean file fragment length for DC2 was 1.9 ± 0.2mm (Figure 23, p. 48).

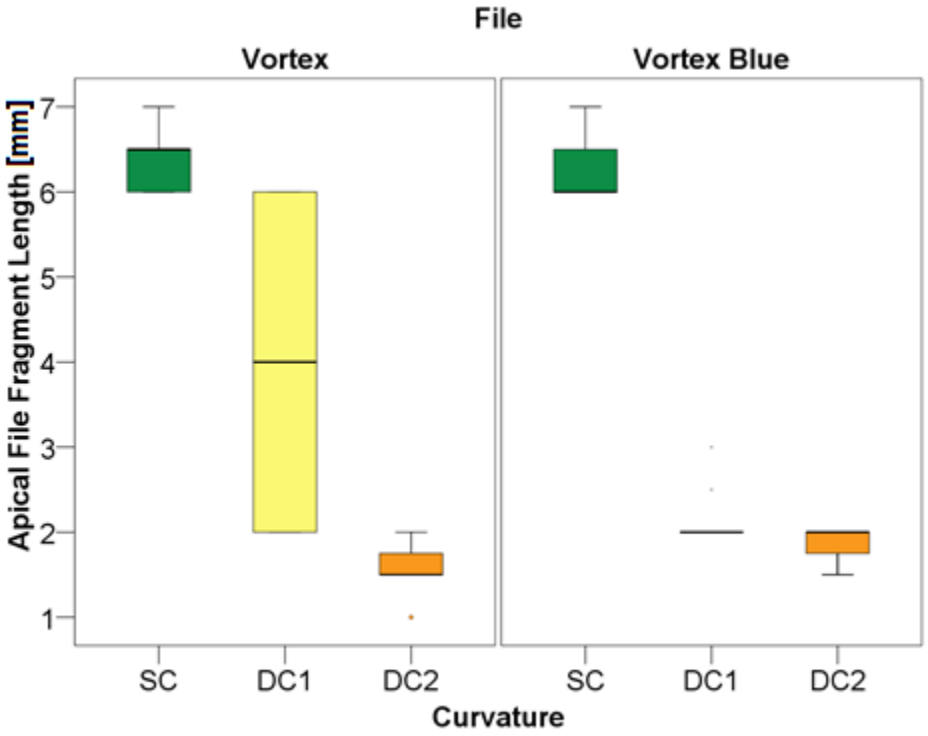

Figure 23. File Fragment Length [mm] for Profile Vortex (VX) (25.04) and Vortex Blue (VB) (25.04) in single curvature (SC), double curvature #1 (DC1) and double curvature #2 (DC2).

Single Curvature

The file type (VX and VB) showed a statistically significant influence on the NCF (Student's t-test; $p < 0.001$). Alternatively, VX and VB had no statistically significant influence on the file fragment length (Mann-Whitney-U test; $p = 0.233$ with Bonferroni correction; $\alpha' = 0.016$).

Double Curvature ONE

The file type (VX and VB) showed no statistically significant influence for both the NCF (Student's t-test; $p = 0.896$) and the file fragment length (Mann-Whitney-U test; $p = 0.037$ with Bonferroni correction; $\alpha' = 0.016$).

Double Curvature TWO

The file type (VX and VB) showed no statistically significant influence for the NCF (Student's t-test; $p = 0.537$). Alternatively, VX and VB had a statistically significant influence on the file fragment length (Mann-Whitney-U test; $p = 0.012$ with Bonferroni correction; $\alpha' = 0.016$).

4.1.3.4 Influence of File Type on Bending Moment

The descriptive data for the file type is presented in Appendix D (Table 7, p. 77).

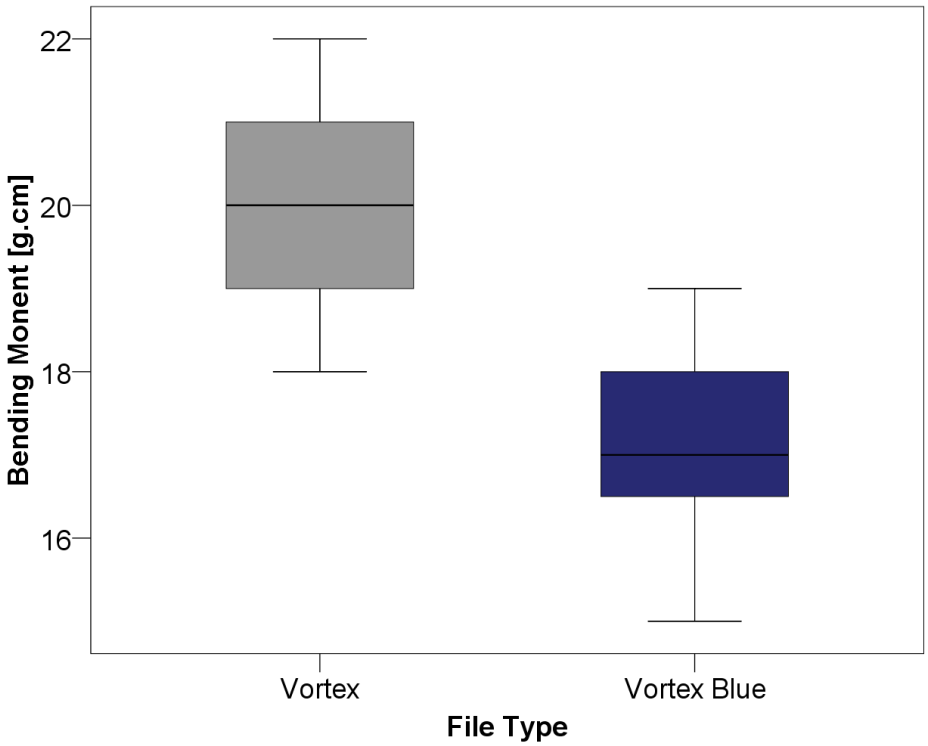

Figure 24. Bending Moment for Profile Vortex (VX) (25.04) and Vortex Blue (VB) (25.04).

The file type (VX and VB) significantly influences the bending moment (Student's t-test-unpaired; $p < 0.001$). VX had a mean bending moment of 20.00 ± 1.13 g·cm and VB had a mean bending moment of 17.08 ± 1.08 g·cm (Figure 24, p. 50). VB is significantly more flexible compared to VX.

4.1.3.5 Fractographic Examination

File fragments were analyzed under Scanning Electron Microscope (SEM) to verify that the file fractured due to cyclic fatigue and not torsional fatigue. All samples showed no signs of torsional fatigue failure and were all considered to have fracture due to cyclic fatigue. Qualitative examination of the SEM images was executed in order to detect any fracture pattern (ex.: number of crack initiation, location of those cracks, etc…). Pictured below are samples of SEM images from each group: SC (Figure 25, p. 52 and Figure 26, p. 53), DC1 (Figure 27, p. 54 and Figure 28, p. 55) and DC2 (Figure 29, p. 56 and Figure 30, p. 57)

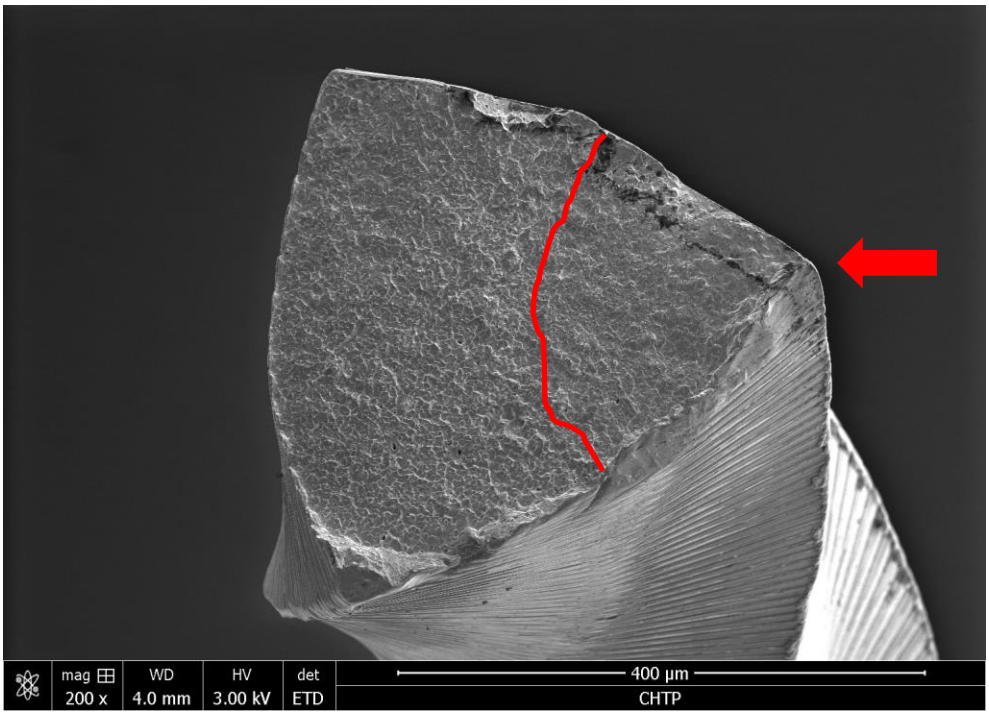

Figure 25. Fractographic examination of VX in the single curvature canal. Red arrow indicates crack initiation location. From arrow to line : chevron pattern zone, and beyond line: zone of rapid crack propagation.

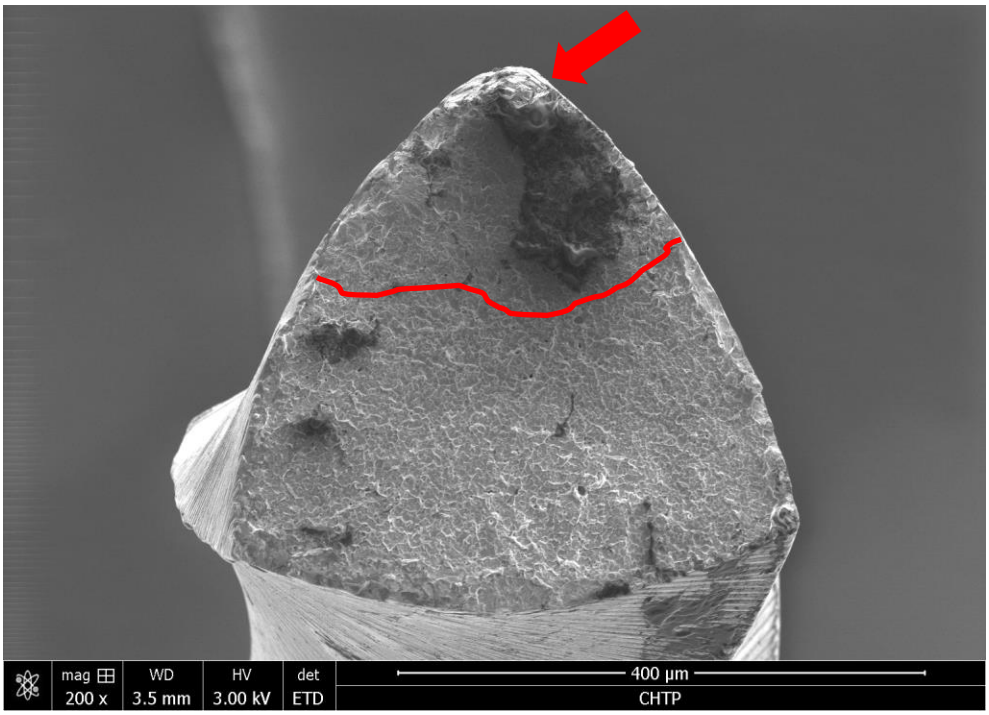

Figure 26. Fractographic examination of VB in the single curvature canal. Red arrow indicates crack initiation location. From arrow to line : chevron pattern zone, and beyond line: zone of rapid crack propagation.

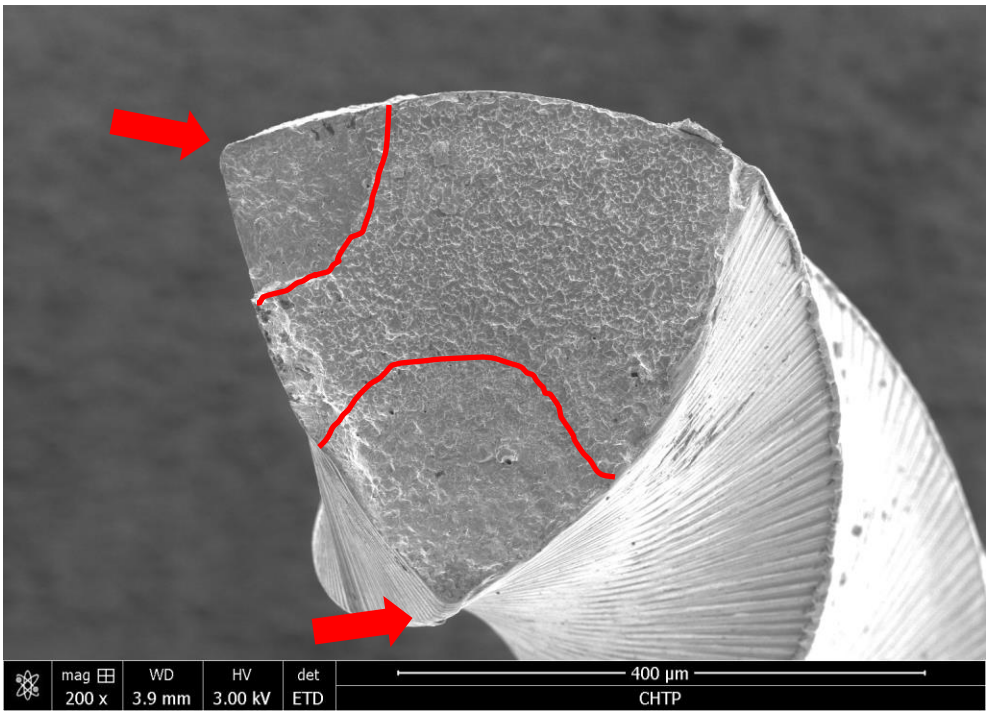

Figure 27. Fractographic examination of VX in the double curvature #1 canal. Red arrow indicates crack initiation location. From arrow to line : chevron pattern zone, and beyond line: zone of rapid crack propagation.

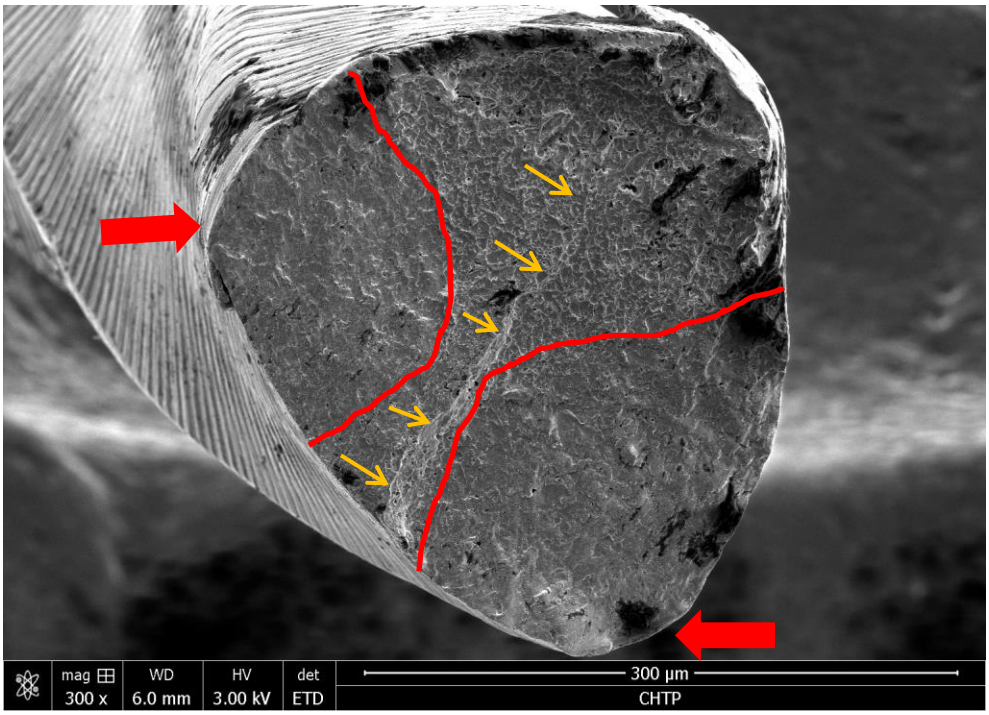

Figure 28. Fractographic examination of VB in the double curvature #1 canal. Red arrow indicates crack initiation location. From arrow to line : chevron pattern zone, and beyond line: zone of rapid crack propagation. Notice the cracks were not on same level longitudinaly along the file's length creating a step where the two crack propagation zones meet (yellow arrows).

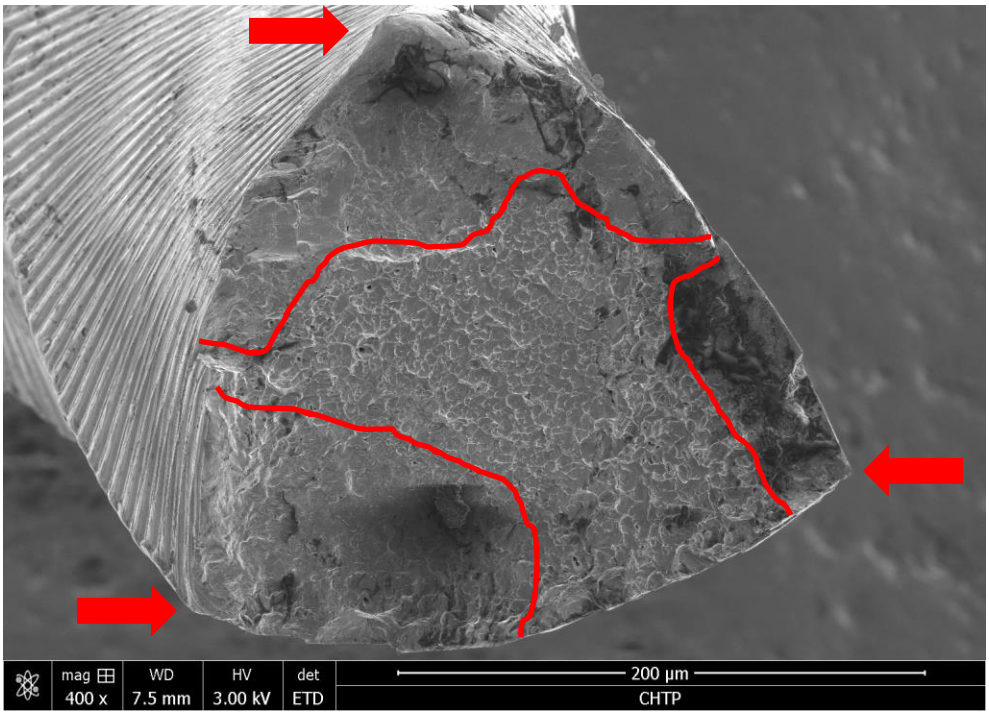

Figure 29. Fractographic examination of VX in the double curvature #2 canal. Red arrow indicates crack initiation location. From arrow to line : chevron pattern zone, and beyond line: zone of rapid crack propagation.

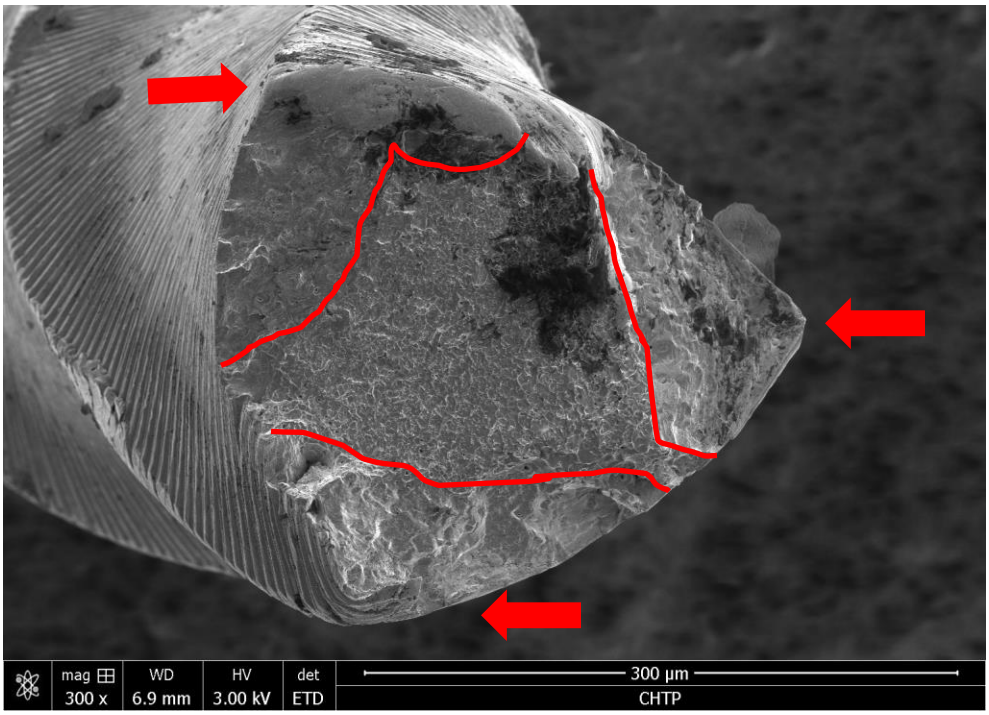

Figure 30. Fractographic examination of VB in the double curvature #2 canal. Red arrow indicates crack initiation location. From arrow to line : chevron pattern zone, and beyond line: zone of rapid crack propagation.

Chapter 5: Discussion

In this study, when the data for all curvatures were combined together, the mean number of cycles to fatigue (NCF) was significantly affected by the file type but the file fragment length was not. The statistical significance for NCF was weak at p=0.044. Curvature, when the data for both files type were combined, significantly affected both the NCF and file fragment length. The influence of the interaction of the two influencing factors (file type and curvature) demonstrated some performance differences between Profile Vortex® and Vortex Blue® in the single curvature only. This is consistent with the result reported by Plotino et al. (59) where Vortex Blue® was able to sustain significantly increased mean NCF before fatigue failure when compared to Profile Vortex®. What is really interesting when we take a closer look at the study mentioned above, is that their parameters for canal curvature are the same as ours in the single curvature (Ø=60°, R=5mm) and they employed a similar machined canal. The authors rotated the same files as in our study (25.04) at 300 rotations per minute (RPM) contrary to the manufacturer's suggested recommendations of 500 RPM (which we followed). The mean value for NCF was similar for Profile Vortex® in both studies but there was a noticeable difference in mean NCF values for Vortex Blue®. As per Young et al. (60), RPM does affect the number of cycles for fatigue failure in situations of low-cycle fatigue ($<10^4$ cycles) (61) and high strain (e.g.: severe curvature) Bardsley et al. (62) found Vortex file to sustain less torque and force when rotated at 400 RPM compared to 200 RPM. In light of that two different RPM were used and other variable were similar (Plotino et al. and this study), one could speculate that the different

thermomechanical treatment received by each file type could explain this difference in mean NCF values for Vortex Blue®.

Many studies (9-12) have demonstrated the presence of double curvature in the root canal system. Clinically, these often go undetected as they are in the same axis as the x-ray beam projecting its image on the image sensor. This study demonstrate a significant reduction ($p < 0.05$) in number of cycles to cyclic fatigue failure (NCF), for both Profile Vortex® and Vortex Blue®, when a simulated canal goes from one curvature to two curvatures. Plotino et al. (57) demonstrated similar results when using Profile ISO® and Profile Vortex®. The single curvature canal configuration was very similar to this study and their double curvature model, although not the same, shared many similarities with the double-curvature #2 canal in our study. Both studies demonstrate the stresses an endodontic file is subjected to when the complexity of the canal is increased to two curvatures. M-Wire® has been shown to sustain higher NCF when compared to conventional nickel-titanium endodontic files (63-67). This was validated in the Al-Sudani et al. (57) study with the single-curvature canal but not with the double-curvature canal despite the clear metallurgic advancement of the M-Wire. In this study, Profile Vortex® and Vortex Blue® showed no advantage over each other in the two double-curvature canals. Profile Vortex® is manufactured with M-Wire® but Vortex Blue® receives post-machining thermomechanical treatment which gives it the distinctive blue color (28). Gao et al. (27) reported a significant increase in NCF for Vortex Blue® versus Profile Vortex® in a moderately single-curved machined canal. Although we duplicated this result in the single-curvature canal, we did not observe any

significant differences in NCF when Profile Vortex® and Vortex Blue® were tested for NCF in either of the two double-curvature canals. Interestingly, Vortex Blue® showed a statistical significant difference in NCF when compared between “double curvature #1” and “double curvature #2”. This was not the case with Profile Vortex® when comparing the two double-curvatures. The mean NCF for each file type decreased as the number of curvatures was added and/or when the complexity of curve wass accentuated. Both Profile Vortex® and Vortex Blue® displayed progressively lower numbers for mean NCF as we look at the data from the single-curvature, then double-curvature #1 and lastly double-curvature #2. With Profile Vortex®, there was an almost directly proportional decrease in mean NCF in relation to the total degrees of curvature in a specific canal (ex.: Profile Vortex® showed half the mean NCF in double curvature #2, with a total of 120° in curvature, when compared to the single curvature, with a total of 60° of curvature in its canal). Vortex Blue® showed similar trends but not as exactly as Profile Vortex® did. Future studies could incorporate a single curvature of 90° and 120° in their protocol in order to compare with the mean NCF data from this study’s double-curvature #1 and #2 canals (total curvature degrees of 90° and 120° respectively). This could help to understand further the effect of canal curvature on the cyclic fatigue failure phenomenon.

Curvature configurations were determined mainly empirically through clinical experience of what constitutes a severely curved or challenging canal anatomy (14, 61, 68). Root canal curvatures present different challenges based on their location along the root canal system (69). We chose to place the more challenging curvatures more apically

as these are often encountered clinically and place an impetus on the clinician to decide what is more important when shaping such root canal anatomies. Different treatment philosophies exist in the endodontic community about the proper apical size in a certain canal should be prepared in order to obtain optimal clinical results. Proponents of a larger apical size are especially faced with the difficult decision of getting a balance from their final shaping sizes and the risk of breaking an endodontic rotary file or an iatrogenic root canal alteration and the challenges of these adverse events bring with them. Canal configurations for this study were also based on previous reports in the literature (55, 56). With the increase in performance of the newer file generations, it is important to place adequate levels of stress on the tested files in order to yield satisfying results. Mild canal curvature or unchallenging root canal anatomy are sometimes not enough to induce file breakage in a reasonable amount of time.

This study is one of the few involving the double curvature canals in its cyclic fatigue failure protocol and highlights the importance of careful pre-operative root canal anatomy assessment. This assessment will guide the clinician on the choice of methods and materials needed for specific cases. File selection is an important factor in general but the newer generations have increased the overall level of safety of their use. In the worst case scenario this study provided (DC2), both files tested lasted on average close to 58 seconds before they fractured. In a multi-step shaping system such as Profile Vortex® and Vortex Blue®, this should be sufficient time for each file to accomplish its shaping duty before fracture. As expressed by some authors (70-72), file fracture during clinical situation is probably a combination of both cyclic fatigue failure

and torsional failure. The close to one-minute time before file fracture in this experiment should not be regarded as a clinical recommendation but more as an upper stress limit in cyclic fatigue failure. The NCF generated from this *in vitro* experiment does not express the full complexity of the clinical situation. The files were tested in a static manner where the stresses from a chosen canal curvature were continuously concentrated at the same level on the files. The experiment was conducted with oil lubrication but in an air environment. Cheung et al. (53) and Shen et al. (73) have demonstrated the improvement on NCF when cyclic fatigue testing is conducted in various aqueous solutions. The lack of downward pressure on the file, the use of static cycle fatigue failure testing model, the lack of root canal material debris due to dentin machining, and the exclusive use of new instruments could have affected either positively or negatively the results gathered in this study. To improve the testing methods in the future, the development of 3-dimensional canal (tube-like) machined to match the geometry of the file to be tested would provide the opportunity to test the file in an aqueous environment with preferably a vertical “up-and-down” motion of the file to simulate a more realistic clinical situation (dynamic testing). Measuring the force needed to place the file in the canal and to move it within the canal during dynamic testing would also provide information in regards of the ease of file insertion in canal and the impact of apical pressure on NCF during cyclic fatigue failure testing.

The fractographic examination confirmed that all file fragments fractured due to cyclic fatigue failure. Although not a direct objective of this study, the fractographic examination of the file fragments’ fractured surfaces revealed the presence of multiple

fracture lines on both Profile Vortex® and Vortex Blue® when subjected to testing in the two double-curvature canals. This could signal a more complex behavior of the nickel-titanium alloys when tested in more challenging root canal anatomy.

Results for the bending moments show similar conclusion as Gao et al. (27) that Vortex Blue® was significantly more flexible than the Profile Vortex® ($p < 0.05$) and could explain the slight variations in file trajectory within the machined root canals. Plotino et al. (55, 56) reported a repeatable and precise file trajectory after machining the root canal 0.1 mm larger than the tested file's dimensions. The trajectory of the files tested in our study varied slightly more but were very close to the desired angulations the machined root canal offered. This could be explained because our canals were machined at a dimension of file tip size #30 with a constant taper of 6%. Both files tested were tip size #25 with constant taper of 4%. In comparison, our model would give closer approximation of the file in the apical half of the canal but would be looser in the coronal half starting at approximately 8-9 mm from the file tip (D8 to D9). This slight change of file trajectory could explain why the Profile Vortex® group in the "double curvature #1" canal showed one-third of them fracturing in the apical curvature (as all other files/double curvatures combinations did) while the other two-thirds fractured in the coronal curvature. The straighter file trajectory of Profile Vortex® in this canal configuration could result in more lateral pressure of the file on the coronal curvature of the canal or that the capability of the larger file diameter in the coronal portion of the canal to resist cyclic fatigue failure was lower than the smaller file diameter in the apical

portion of the canal even though the coronal curvature and its radius were gentler than the apical one.

Chapter 6: Conclusion

Within the limitations of this *in vitro* study, it was demonstrated that Vortex Blue® was statistically more resistant to cyclic fatigue failure when compared to Profile Vortex® only in the single curvature canal. Both Profile Vortex® and Vortex Blue® were significantly affected by the addition of any of the two second apical curvature in the canal system compared to the single curvature canal. No statistical differences in mean NCF could be measured between the two file types when they were tested in the two double-curvature canal configurations. Bending moment data showed that Vortex Blue® was significantly more flexible than Profile Vortex® and would explain the file trajectory variations between the two file types within the same canal configuration and the different locations of file fracture within the Profile Vortex® group used in the "double-curvature #1" canal. Even when these changes in trajectory are noted, this study managed to rule out many confounding factors between the two files used. Size, taper, length, geometry and design were the same for both files. The only factor distinguishing the two files was their respective thermomechanical treatment during the manufacturing process.

The first null hypothesis mentioned earlier in this document was partially rejected. It stated that the different thermomechanical treatment used for each file would not affect the NCF in each canal curvature scenario. In fact, the two files only affected significantly the NCF when they were tested in the single-curvature canal but not in the two double-curvature canals. The second hypothesis stated that the NCF would not be affected by single- or double-curvature canals. This hypothesis was rejected as both files showed

statistical differences between single- and double-curvature canals. Interestingly, when focusing on the two double-curvature canals, only Vortex Blue® showed a statistical difference between the two canal configurations but not so with Profile Vortex®.

In conclusion, despite the previous claims of superior performance in regards of NCF of Vortex Blue® over Profile Vortex® when used in the single curvature, this did not translate into double-curvature canal configurations. Double-curvature canal configurations demonstrated the effect of canal curvature and its radius on the complex pattern of file fracture when canal anatomy is more challenging. The flexibility of an endodontic file could also be a factor in determining its NCF. The clinician should always be on the lookout for potential severe changes in the root canal anatomy prior and during root canal therapy and expect potential root canal shaping difficulties even when the radiographs are seemingly within normal limits.

Bibliography

1. Cruse WP, Bellizzi R. A historic review of endodontics, 1689-1963, part 1. Journal of endodontics 1980;6(3):495-499.

2. Zinelis S, Magnissalis EA, Margelos J, Lambrianidis T. Clinical relevance of standardization of endodontic files dimensions according to the ISO 3630-1 specification. Journal of endodontics 2002;28(5):367-370.

3. Buehler W, Gilfrich J, Wiley R. Effect of low temperature phase change on the mechanical properties of alloys near composition NiTi. Journal of Applied Physics 1963;34(5):1475-1477.

4. Buehler W, Wiley R. The properties of Ni-Ti and associated phases. US Naval Ordinance Lab. Tech. Report 61 1961.

5. Andreasen GF, Morrow RE. Laboratory and clinical analyses of nitinol wire. American journal of orthodontics 1978;73(2):142-151.

6. Walia HM, Brantley WA, Gerstein H. An initial investigation of the bending and torsional properties of Nitinol root canal files. Journal of endodontics 1988;14(7):346-351.

7. Hülsmann M, Peters OA, Dummer PM. Mechanical preparation of root canals: shaping goals, techniques and means. Endodontic Topics 2005;10:30-76.

8. Schilder H. Cleaning and shaping the root canal. Dental clinics of North America 1974;18(2):269-296.

9. Cunningham CJ, Senia ES. A three-dimensional study of canal curvatures in the mesial roots of mandibular molars. Journal of endodontics 1992;18(6):294-300.

10. Willershausen B, Kasaj A, Tekyatan H, Roehrig B, Briseno B. Radiographic investigation of location and angulation of curvatures in human maxillary incisors. Journal of endodontics 2008;34(9):1052-1056.

11. Willershausen B, Tekyatan H, Kasaj A, Marroquin BB. Roentgenographic in vitro investigation of frequency and location of curvatures in human maxillary premolars. Journal of endodontics 2006;32(4):307-311.

12. Schafer E, Diez C, Hoppe W, Tepel J. Roentgenographic investigation of frequency and degree of canal curvatures in human permanent teeth. Journal of endodontics 2002;28(3):211-216.

13. Schneider SW. A comparison of canal preparations in straight and curved root canals. Oral surgery, oral medicine, and oral pathology 1971;32(2):271-275.

14. Pruett JP, Clement DJ, Carnes DL, Jr. Cyclic fatigue testing of nickel-titanium endodontic instruments. Journal of endodontics 1997;23(2):77-85.

15. Tan BT, Messer HH. The quality of apical canal preparation using hand and rotary instruments with specific criteria for enlargement based on initial apical file size. Journal of endodontics 2002;28(9):658-664.

16. De-Deus G, Garcia-Filho P. Influence of the NiTi rotary system on the debridement quality of the root canal space. Oral surgery, oral medicine, oral pathology, oral radiology, and endodontics 2009;108(4):e71-76.

17. Brunson M, Heilborn C, Johnson DJ, Cohenca N. Effect of apical preparation size and preparation taper on irrigant volume delivered by using negative pressure irrigation system. Journal of endodontics 2010;36(4):721-724.

18. Arvaniti IS, Khabbaz MG. Influence of root canal taper on its cleanliness: a scanning electron microscopic study. Journal of endodontics 2011;37(6):871-874.

19. de Gregorio C, Arias A, Navarrete N, Del Rio V, Oltra E, Cohenca N. Effect of apical size and taper on volume of irrigant delivered at working length with apical negative pressure at different root curvatures. Journal of endodontics 2013;39(1):119-124.

20. Thompson SA. An overview of nickel-titanium alloys used in dentistry. International endodontic journal 2000;33(4):297-310.

21. Zhou H, Peng B, Zheng Y. An overview of the mechanical properties of nickel-titanium endodontic instruments. Endodontic Topics 2013;29:42-54.

22. Baumann MA. Nickel-titanium: options and challenges. Dental clinics of North America 2004;48(1):55-67.

23. Haapasalo M, Shen Y. Evolution of nickel-titanium instruments: from past to future. Endodontic Topics 2013;29:3-17.

24. Peters OA, Paque F. Current developments in rotary root canal instrument technology and clinical use: a review. Quintessence Int 2010;41(6):479-488.

25. Shen Y, Zhou HM, Zheng YF, Peng B, Haapasalo M. Current challenges and concepts of the thermomechanical treatment of nickel-titanium instruments. Journal of endodontics 2013;39(2):163-172.

26. Berutti E, Chiandussi G, Gaviglio I, Ibba A. Comparative analysis of torsional and bending stresses in two mathematical models of nickel-titanium rotary instruments: ProTaper versus ProFile. Journal of endodontics 2003;29(1):15-19.

27. Gao Y, Gutmann JL, Wilkinson K, Maxwell R, Ammon D. Evaluation of the impact of raw materials on the fatigue and mechanical properties of ProFile Vortex rotary instruments. Journal of endodontics 2012;38(3):398-401.

28. Shen Y, Zhou H, Coil JM, Aljazaeri B, Buttar R, Wang Z, et al. ProFile Vortex and Vortex Blue Nickel-Titanium Rotary Instruments after Clinical Use. Journal of endodontics 2015;41(6):937-942.

29. Bradley TG, Brantley WA, Culbertson BM. Differential scanning calorimetry (DSC) analyses of superelastic and nonsuperelastic nickel-titanium orthodontic wires. American journal of orthodontics and dentofacial orthopedics : official publication of the American Association of Orthodontists, its constituent societies, and the American Board of Orthodontics 1996;109(6):589-597.

30. Brantley WA, Svec TA, Iijima M, Powers JM, Grentzer TH. Differential scanning calorimetric studies of nickel titanium rotary endodontic instruments. Journal of endodontics 2002;28(8):567-572.

31. Schafer E, Dammaschke T. Development and sequelae of canal transportation. Endodontic Topics 2009;15:75-90.

32. Cheung GS, Liu CS. A retrospective study of endodontic treatment outcome between nickel-titanium rotary and stainless steel hand filing techniques. Journal of endodontics 2009;35(7):938-943.

33. Yared GM, Bou Dagher FE, Machtou P. Influence of rotational speed, torque and operator's proficiency on ProFile failures. International endodontic journal 2001;34(1):47-53.

34. Yared GM, Dagher FE, Machtou P, Kulkarni GK. Influence of rotational speed, torque and operator proficiency on failure of Greater Taper files. International endodontic journal 2002;35(1):7-12.

35. Di Fiore PM. A dozen ways to prevent nickel-titanium rotary instrument fracture. J Am Dent Assoc 2007;138(2):196-201; quiz 249.

36. Cheung GS. Instrument fracture: mechanisms, removal of fragments, and clinical outcomes. Endodontic Topics 2009;16:1-26.

37. Arens FC, Hoen MM, Steiman HR, Dietz GC, Jr. Evaluation of single-use rotary nickel-titanium instruments. Journal of endodontics 2003;29(10):664-666.

38. Spili P, Parashos P, Messer HH. The impact of instrument fracture on outcome of endodontic treatment. Journal of endodontics 2005;31(12):845-850.

39. Parashos P, Messer HH. Rotary NiTi instrument fracture and its consequences. Journal of endodontics 2006;32(11):1031-1043.

40. Cohen S, Berman LH, Blanco L, Bakland L, Kim JS. A demographic analysis of vertical root fractures. Journal of endodontics 2006;32(12):1160-1163.

41. Tsujimoto M, Irifune Y, Tsujimoto Y, Yamada S, Watanabe I, Hayashi Y. Comparison of conventional and new-generation nickel-titanium files in regard to their physical properties. Journal of endodontics 2014;40(11):1824-1829.

42. Sattapan B, Nervo GJ, Palamara JE, Messer HH. Defects in rotary nickel-titanium files after clinical use. Journal of endodontics 2000;26(3):161-165.

43. Cheung GS, Peng B, Bian Z, Shen Y, Darvell BW. Defects in ProTaper S1 instruments after clinical use: fractographic examination. International endodontic journal 2005;38(11):802-809.

44. Cheung GS, Darvell BW. Fatigue testing of a NiTi rotary instrument. Part 2: Fractographic analysis. International endodontic journal 2007;40(8):619-625.

45. Campbell L, Shen Y, Zhou HM, Haapasalo M. Effect of fatigue on torsional failure of nickel-titanium controlled memory instruments. Journal of endodontics 2014;40(4):562-565.

46. Shen Y, Cheung GS. Methods and models to study nickel-titanium instruments. Endodontic Topics 2013;29:18-41.

47. Plotino G, Grande NM, Cordaro M, Testarelli L, Gambarini G. A review of cyclic fatigue testing of nickel-titanium rotary instruments. Journal of endodontics 2009;35(11):1469-1476.

48. Haikel Y, Serfaty R, Bateman G, Senger B, Allemann C. Dynamic and cyclic fatigue of engine-driven rotary nickel-titanium endodontic instruments. Journal of endodontics 1999;25(6):434-440.

49. Li UM, Lee BS, Shih CT, Lan WH, Lin CP. Cyclic fatigue of endodontic nickel titanium rotary instruments: static and dynamic tests. Journal of endodontics 2002;28(6):448-451.

50. Lopes HP, Britto IM, Elias CN, Machado de Oliveira JC, Neves MA, Moreira EJ, et al. Cyclic fatigue resistance of ProTaper Universal instruments when subjected to static and dynamic tests. Oral surgery, oral medicine, oral pathology, oral radiology, and endodontics 2010;110(3):401-404.

51. Cheung GS, Shen Y, Darvell BW. Does electropolishing improve the low-cycle fatigue behavior of a nickel-titanium rotary instrument in hypochlorite? Journal of endodontics 2007;33(10):1217-1221.
52. Cheung GS, Darvell BW. Fatigue testing of a NiTi rotary instrument. Part 1: Strain-life relationship. International endodontic journal 2007;40(8):612-618.

53. Cheung GS, Shen Y, Darvell BW. Effect of environment on low-cycle fatigue of a nickel-titanium instrument. Journal of endodontics 2007;33(12):1433-1437.

54. Grande NM, Plotino G, Pecci R, Bedini R, Malagnino VA, Somma F. Cyclic fatigue resistance and three-dimensional analysis of instruments from two nickel-titanium rotary systems. International endodontic journal 2006;39(10):755-763.

55. Plotino G, Grande NM, Cordaro M, Testarelli L, Gambarini G. Measurement of the trajectory of different NiTi rotary instruments in an artificial canal specifically designed for cyclic fatigue tests. Oral surgery, oral medicine, oral pathology, oral radiology, and endodontics 2009;108(3):e152-156.

56. Plotino G, Grande NM, Mazza C, Petrovic R, Testarelli L, Gambarini G. Influence of size and taper of artificial canals on the trajectory of NiTi rotary instruments in cyclic fatigue studies. Oral surgery, oral medicine, oral pathology, oral radiology, and endodontics 2010;109(1):e60-66.

57. Al-Sudani D, Grande NM, Plotino G, Pompa G, Di Carlo S, Testarelli L, et al. Cyclic fatigue of nickel-titanium rotary instruments in a double (S-shaped) simulated curvature. Journal of endodontics 2012;38(7):987-989.

58. Standardization. IOf. International Organization for Standardization. Dentistry-Root canal files-Part 1: General Requirements and Test Methods. ISO; 2008: 3630-1. . 2008.

59. Plotino G, Grande NM, Cotti E, Testarelli L, Gambarini G. Blue treatment enhances cyclic fatigue resistance of vortex nickel-titanium rotary files. Journal of endodontics 2014;40(9):1451-1453.

60. Young JM, Van Vliet KJ. Predicting in vivo failure of pseudoelastic NiTi devices under low cycle, high amplitude fatigue. Journal of biomedical materials research. Part B, Applied biomaterials 2005;72(1):17-26.

61. Rodrigues RC, Lopes HP, Elias CN, Amaral G, Vieira VT, De Martin AS. Influence of different manufacturing methods on the cyclic fatigue of rotary nickel-titanium endodontic instruments. Journal of endodontics 2011;37(11):1553-1557.

62. Bardsley S, Peters CI, Peters OA. The effect of three rotational speed settings on torque and apical force with vortex rotary instruments in vitro. Journal of endodontics 2011;37(6):860-864.

63. Johnson E, Lloyd A, Kuttler S, Namerow K. Comparison between a novel nickel-titanium alloy and 508 nitinol on the cyclic fatigue life of ProFile 25/.04 rotary instruments. Journal of endodontics 2008;34(11):1406-1409.

64. Al-Hadlaq SM, Aljarbou FA, AlThumairy RI. Evaluation of cyclic flexural fatigue of M-wire nickel-titanium rotary instruments. Journal of endodontics 2010;36(2):305-307.

65. Gao Y, Shotton V, Wilkinson K, Phillips G, Johnson WB. Effects of raw material and rotational speed on the cyclic fatigue of ProFile Vortex rotary instruments. Journal of endodontics 2010;36(7):1205-1209.

66. Ye J, Gao Y. Metallurgical characterization of M-Wire nickel-titanium shape memory alloy used for endodontic rotary instruments during low-cycle fatigue. Journal of endodontics 2012;38(1):105-107.

67. Pereira ES, Gomes RO, Leroy AM, Singh R, Peters OA, Bahia MG, et al. Mechanical behavior of M-Wire and conventional NiTi wire used to manufacture rotary endodontic instruments. Dent Mater 2013;29(12):e318-324.

68. Inan U, Aydin C, Tunca YM. Cyclic fatigue of ProTaper rotary nickel-titanium instruments in artificial canals with 2 different radii of curvature. Oral surgery, oral medicine, oral pathology, oral radiology, and endodontics 2007;104(6):837-840.

69. Lopes HP, Vieira MV, Elias CN, Goncalves LS, Siqueira JF, Jr., Moreira EJ, et al. Influence of the geometry of curved artificial canals on the fracture of rotary nickel-titanium instruments subjected to cyclic fatigue tests. Journal of endodontics 2013;39(5):704-707.

70. Kim HC, Cheung GS, Lee CJ, Kim BM, Park JK, Kang SI. Comparison of forces generated during root canal shaping and residual stresses of three nickel-titanium rotary files by using a three-dimensional finite-element analysis. Journal of endodontics 2008;34(6):743-747.

71. Blum JY, Machtou P, Ruddle C, Micallef JP. Analysis of mechanical preparations in extracted teeth using ProTaper rotary instruments: value of the safety quotient. Journal of endodontics 2003;29(9):567-575.

72. Sattapan B, Palamara JE, Messer HH. Torque during canal instrumentation using rotary nickel-titanium files. Journal of endodontics 2000;26(3):156-160.

73. Shen Y, Qian W, Abtin H, Gao Y, Haapasalo M. Effect of environment on fatigue failure of controlled memory wire nickel-titanium rotary instruments. Journal of endodontics 2012;38(3):376-380.

Appendices

Appendix A - Influencing Factor - File Type

Descriptive Statistics for NCF

Table 1. Descriptive statistics for number of cycles for failure (NCF).

	NCF	
	Profile Vortex®	**Vortex Blue®**
Mean	660.2	710.7
Median	558.5	604.5
Variance	47699.3	68157.2
Standard Deviation	218.4	261.1
Minimum	375.0	375.0
Maximum	1025.0	1167.0
Interquartile Range	411.0	542.0

Descriptive Statistics for Apical Fragment Length

Table 2. Descriptive statistics for apical fragment length (mm).

	Fragment Length (mm)	
	Profile Vortex®	**Vortex Blue®**
Mean	4.0	3.4
Median	4.0	2.0
Variance	5.5	4.1
Standard Deviation	2.3	2.0
Minimum	1.0	1.5
Maximum	7.0	7.0
Interquartile Range	4.4	4.0

Appendix B - Influencing factor – Canal Curvature

Descriptive Statistics for NCF

Table 3. Descriptive statistics for number of cycles to failure (NCF).

	NCF		
	Single curvature (SC)	**Double curvature #1 (DC1)**	**Double curvature #2 (DC2)**
Mean	978.5	598.4	479.5
Median	971.0	554.5	479.0
Variance	11823.5	19428.5	5228.0
Standard Deviation	108.7	139.4	72.3
Minimum	700.0	383.0	375.0
Maximum	1167.0	942.0	683.0
Interquartile Range	146.0	148.0	94.0

Descriptive Statistics for Apical Fragment Length

Table 4. Descriptive statistics for apical fragment length (mm).

	Fragment Length (mm)		
	Single curvature (SC)	**Double curvature #1 (DC1)**	**Double curvature #2 (DC2)**
Mean	6.3	3.1	1.7
Median	6.0	2.0	1.7
Variance	0.1	3.0	0.1
Standard Deviation	0.4	1.7	0.3
Minimum	6.0	2.0	1.0
Maximum	7.0	6.0	2.0
Interquartile Range	0.5	3.3	0.5

Appendix C - Influencing Factor - Interaction of File Type and Canal Curvature

Descriptive Statistics for NCF

Table 5. Descriptive statistics for number of cycles to fatigue (NCF).

	NCF					
	Profile Vortex®			Vortex Blue®		
	SC	DC1	DC2	SC	DC1	DC2
Mean	908.3	602.2	470.1	1048.7	594.6	488.8
Median	933.0	554.5	500.0	1067.0	567.0	471.0
Variance	8529.9	29654.9	3324.4	5437.3	10936.3	7415.1
Standard Deviation	92.4	172.2	57.7	73.7	104.6	86.1
Minimum	700.0	383.0	375.0	917.0	483.0	375.0
Maximum	1025.0	942.0	550.0	1167.0	817.0	683.0
Interquartile Range	19.0	165.0	87.0	100.0	167.0	132.0

Single curvature (SC), double curvature #1 (DC1) and double curvature #2 (DC2).

Descriptive Statistics for Apical Fragment Length

Table 6. Descriptive statistics for apical fragment length.

	Fragment Length (mm)					
	Profile Vortex®			Vortex Blue®		
	SC	DC1	DC2	SC	DC1	DC2
Mean	6.4	4.0	1.5	6.2	2.1	1.9
Median	6.5	4.0	1.5	6.0	2.0	2.0
Variance	0.1	4.4	0.1	0.1	0.1	0.0
Standard Deviation	0.4	2.1	0.3	0.3	0.3	0.2
Minimum	6.0	2.0	1.0	6.0	2.0	1.5
Maximum	7.0	6.0	2.0	7.0	3.0	2.0
Interquartile Range	0.5	4.0	0.4	0.5	0.0	0.4

Single curvature (SC), double curvature #1 (DC1) and double curvature #2 (DC2).

Appendix D - Influence of File Type on Bending Moment

Descriptive Statistics for Bending Moment

Table 7. Descriptive statistics for bending moment (g·cm).

	Bending Moment (g·cm)	
	Profile Vortex®	**Vortex Blue®**
Mean	20.00	17.08
Median	20.00	17.00
Variance	1.27	1.17
Standard Deviation	1.13	1.08
Minimum	18	15
Maximum	22	19
Interquartile Range	2	2

Appendix E - Results Chart

Table 8. Results chart.

Files (500 rpm)	Bending Moment (g·cm)	Single Curvature (Θ=60° R=5mm)		Double Curvature 1 (Θ1 =60°, R1=5mm; Θ2=30°, R2=2mm)		Double Curvature 2 (Θ1 =60°, R1=5mm; Θ2=60°, R2=2mm)	
		NCF	Length (mm)	NCF	Length (mm)	NCF	Length (mm)
Profile Vortex	20.0±1.1$^{\triangle}$	908.3 ± 92.4^{a}	6.4 ± 0.4^{A}	602.2 ± 172.2^{c}	4.0 ± 2.1^{B}	470.1 ± 57.7^{c,d}	1.5 ± 0.3^{C}
Vortex Blue	17.1±1.1$^{\lozenge}$	1048.7 ±73.7^{b}	6.2 ± 0.3^{A}	594.6 ± 104.6^{c}	2.1 ± 0.3^{B}	488.8 ± 86.1^{d}	1.9 ± 0.2^{B,D}

Two-way ANOVA, $p<0.05$

NCF: Number of Cycles for Fracture

For bending moment: Different superscript indicate a statistical significance ($p<0.05$).

For NCF: Different superscript (lower case letters) indicate a statistical significance ($p<0.05$).

For fragment length (length): Different superscript (upper case letters) indicate a statistical significance ($p<0.05$).